O. Niedermaier, PRL 94 172501 (2005)

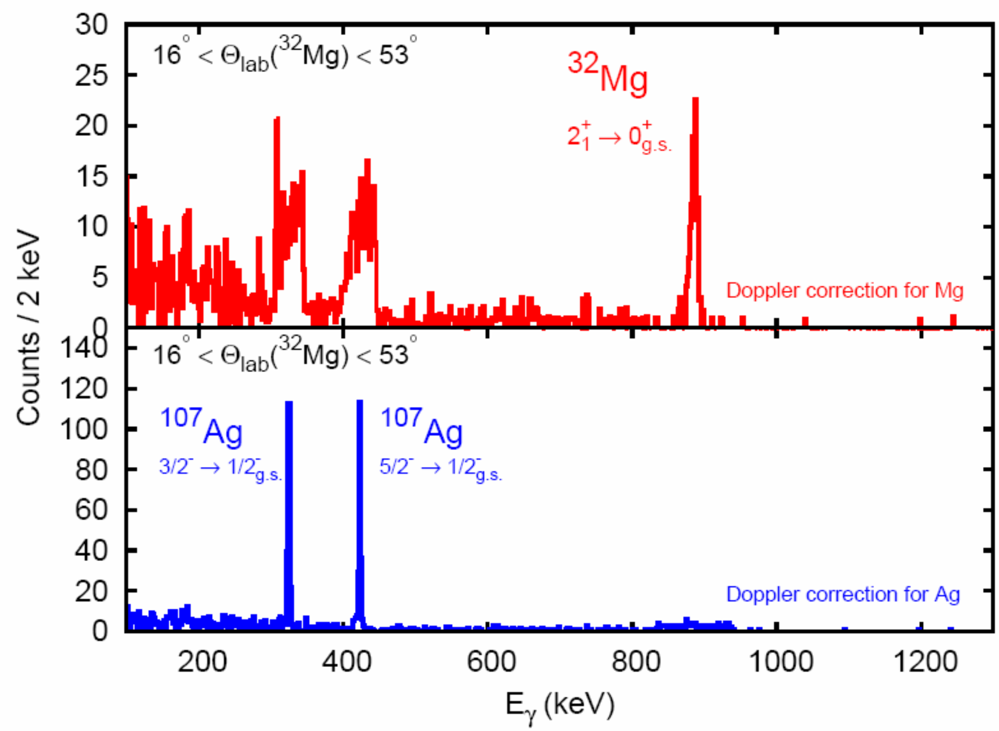

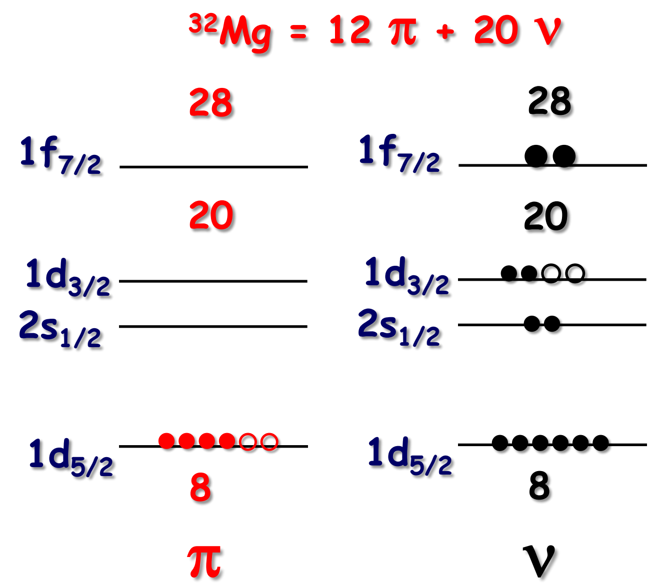

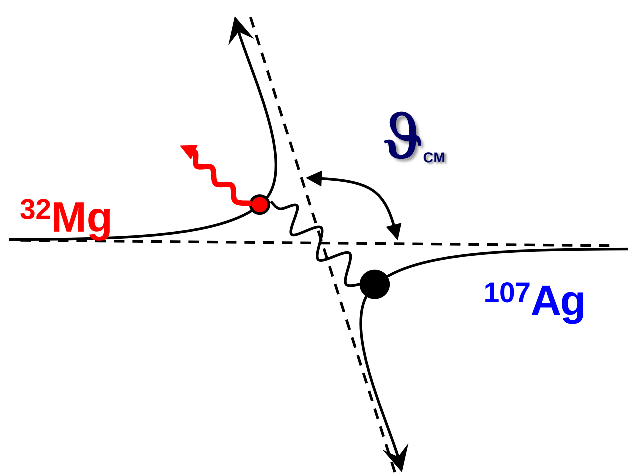

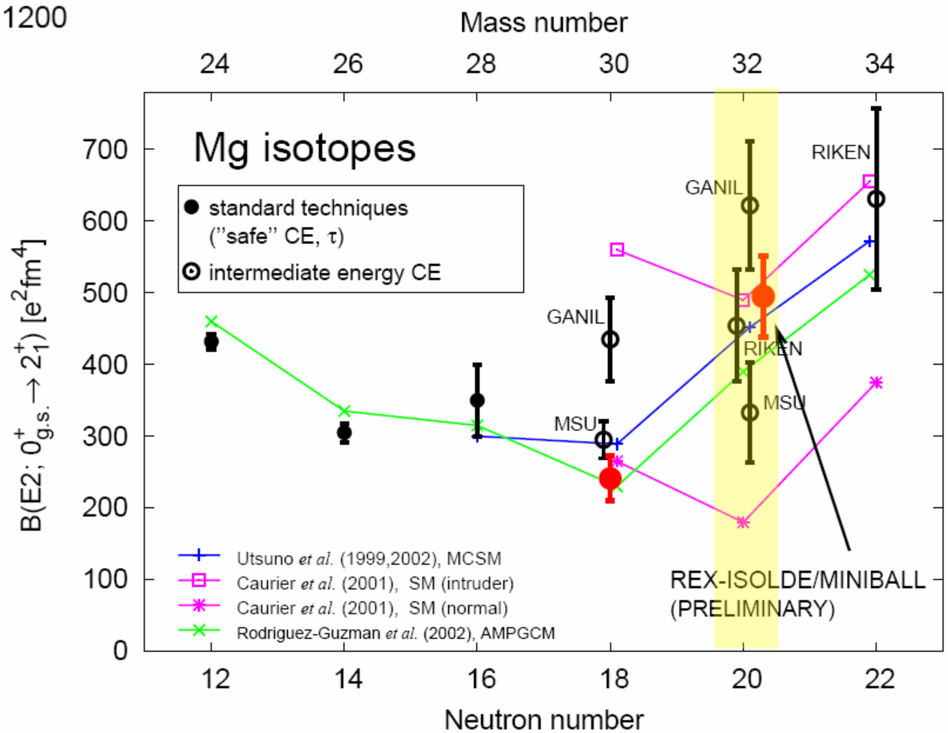

Island of Inversion: Open questions

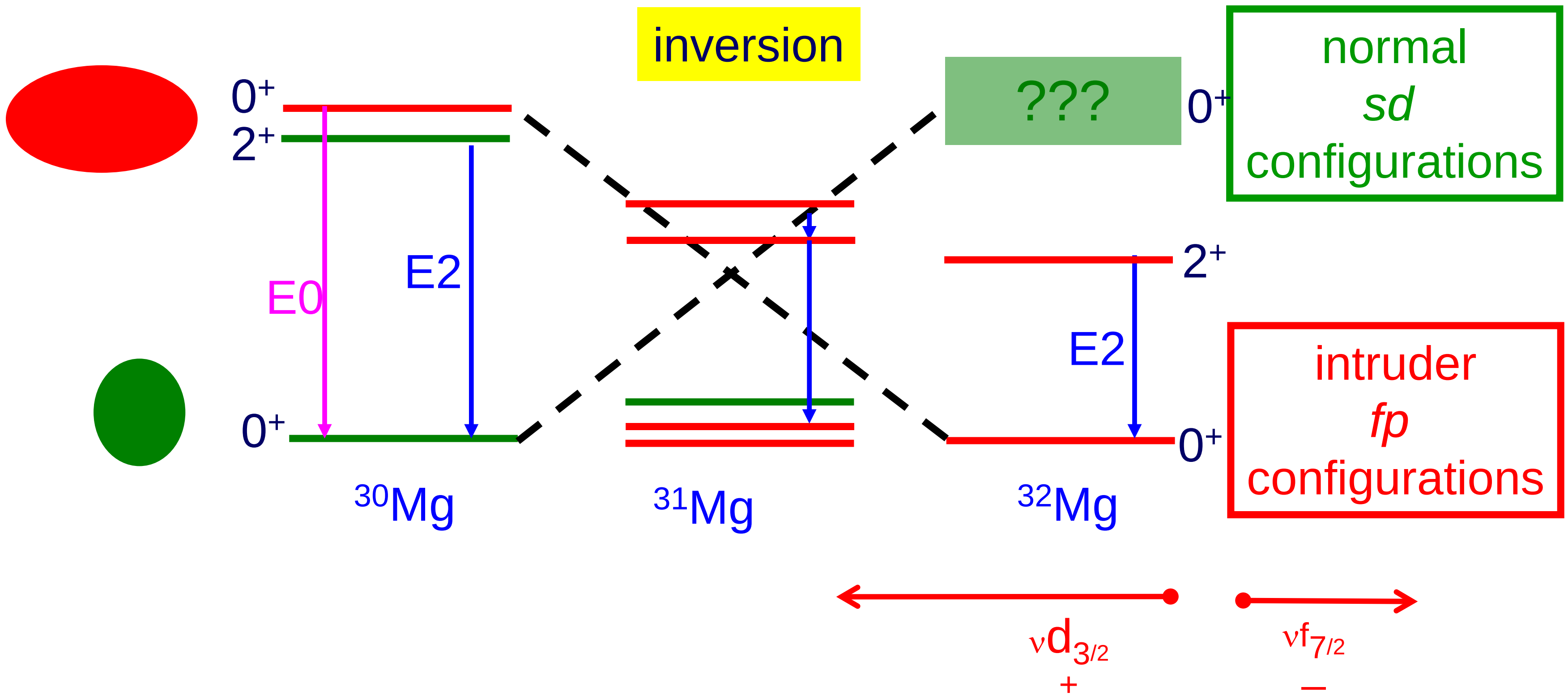

- Where are the borders?
- How does transition into island of inversion occur ?
- Does picture of shape coexistence hold?

g-factor and spin of the ^{31,33}Mg ground state

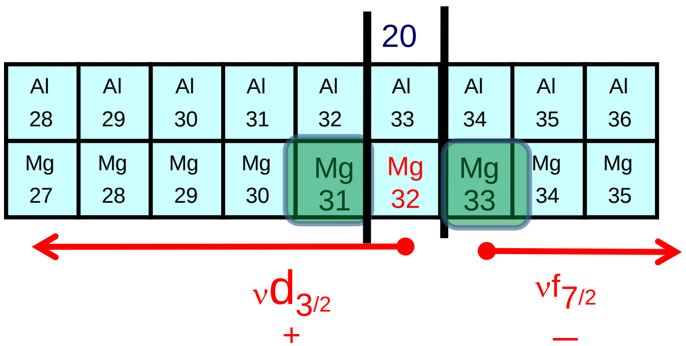

laser spectroscopy and β-NMR
g-factor and spin for ^{31}Mg and ^{33}Mg
from sign of g-factor → parity

^{31}Mg, $I^{\pi} = 1/2^{+}$ $\nu(sd)^{-3}(fp)^{2}$
^{33}Mg, $I^{\pi} = 3/2^{-}$ $\nu(sd)^{-2}(fp)^{3}$

→ pure 2p-2h intruder ground states !

Intruder ground state configurations:

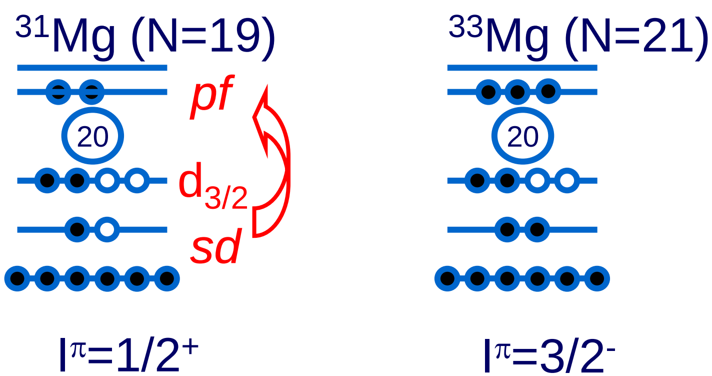

Normal ground state configurations:

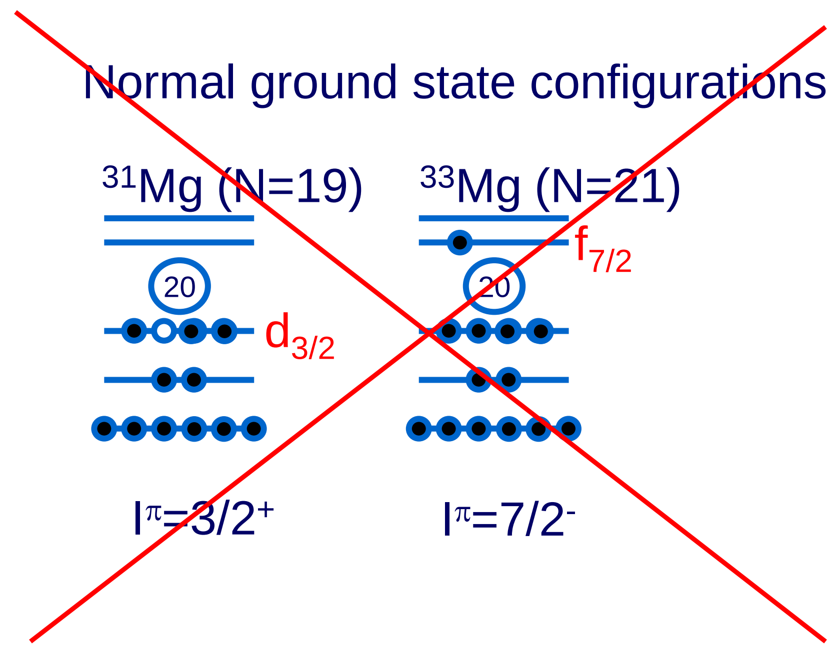

G. Neyens et al., PRL 94, 022501 (2005)
D. Yordanov et al., PRL 99, 212501 (2007)

Coulomb excitation ^{31}Mg

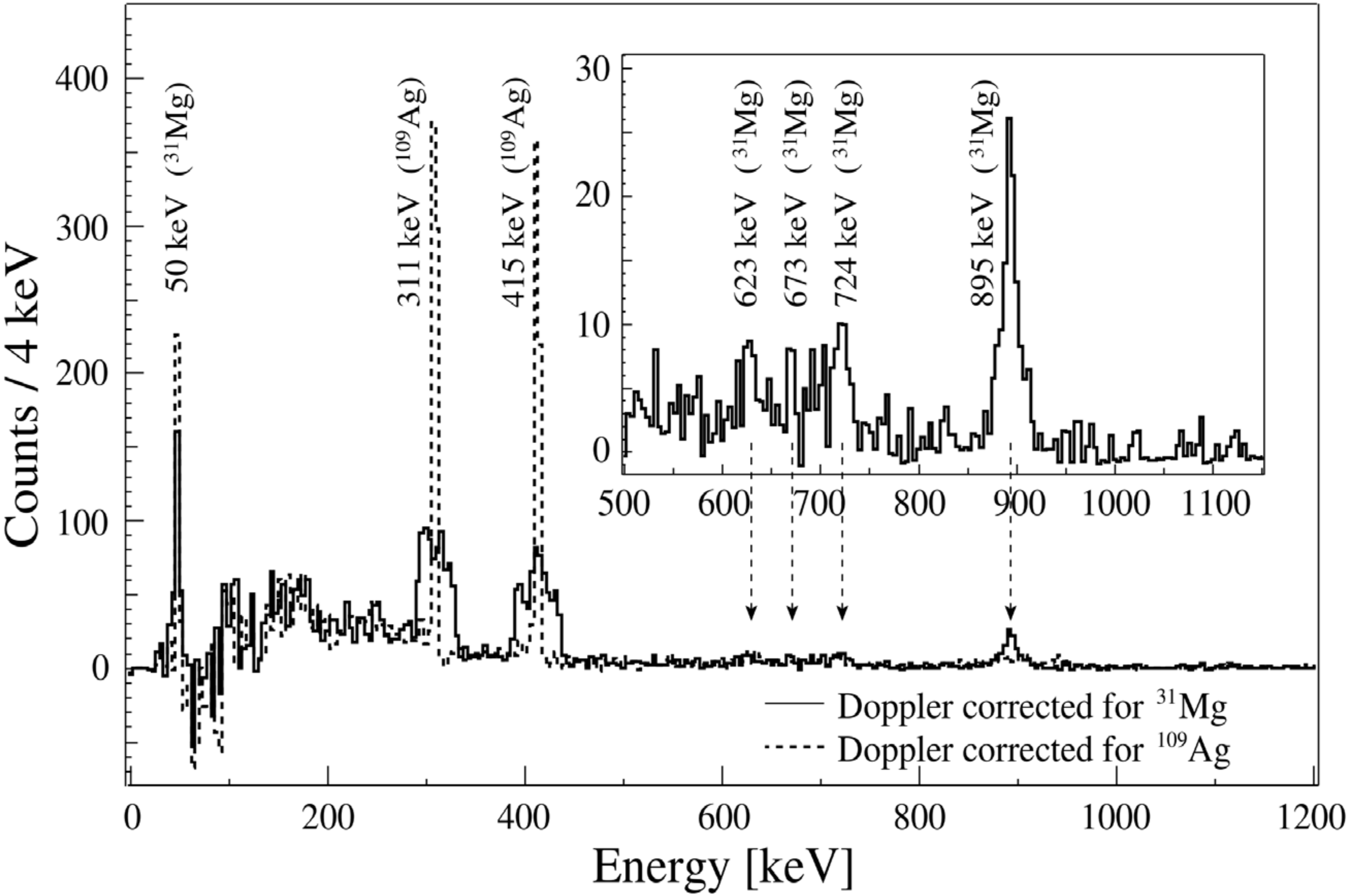

GOSIA Coulomb excitation calculation

Results:

- one step E2 excitation

$$B(E2,\ 1/2^+ \rightarrow 5/2^+) = 182\ e^2fm^4$$

- decay of (5/2+,3/2+) level via M1 transition

$$B(M1,\ 5/2^+ \rightarrow 3/2^+) = 0.1 - 0.5\ \mu_n^2$$

- results confirms strong collective excitation
- rotational sequence: $1/2^+ \rightarrow 3/2^+ \rightarrow 5/2^+$

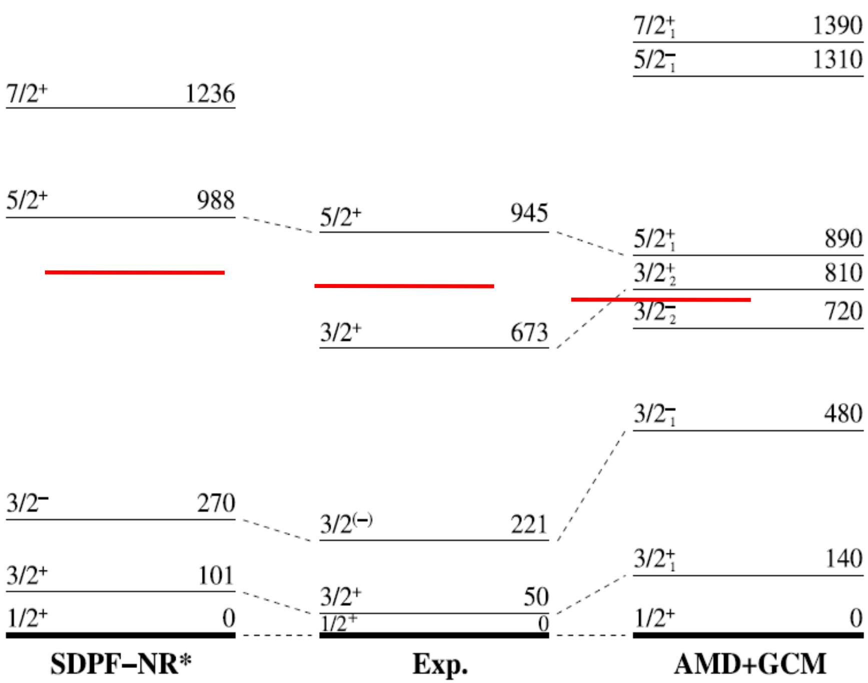

M. Kimura, Phys. Rev. C 75, 041302(R) (2007)

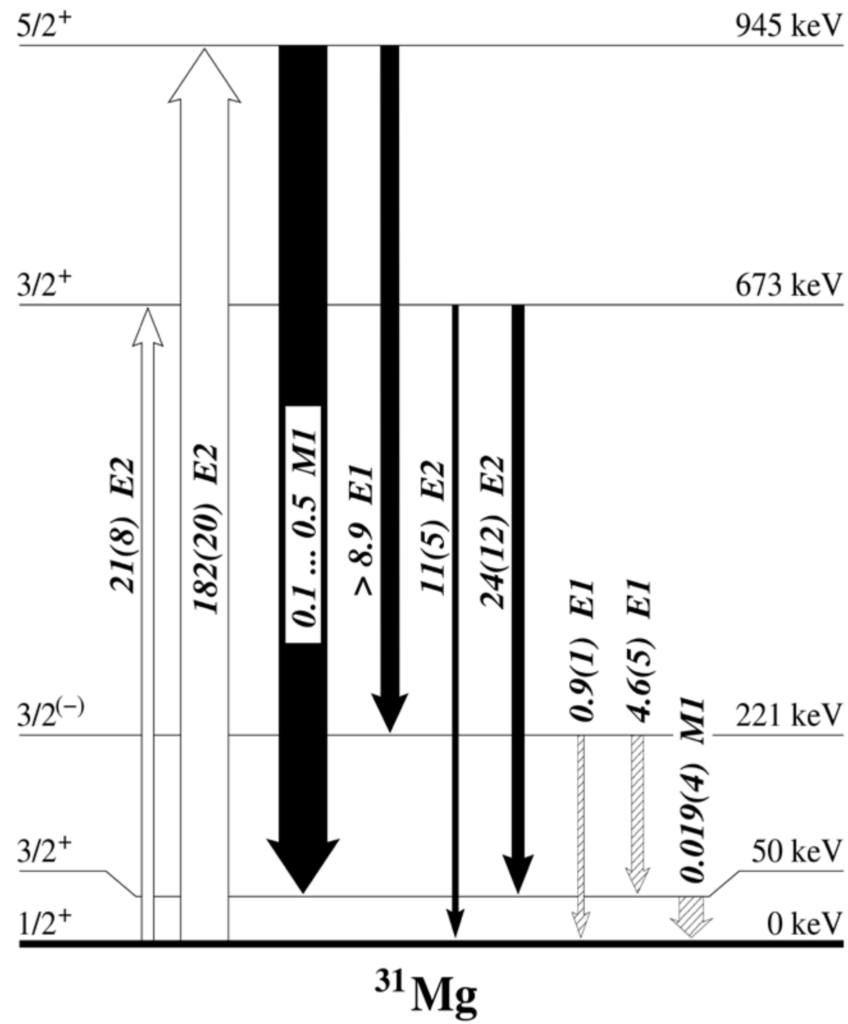

M. Seidlitz et al; PLB 700 (2011) 181

Summary:Island of inversion

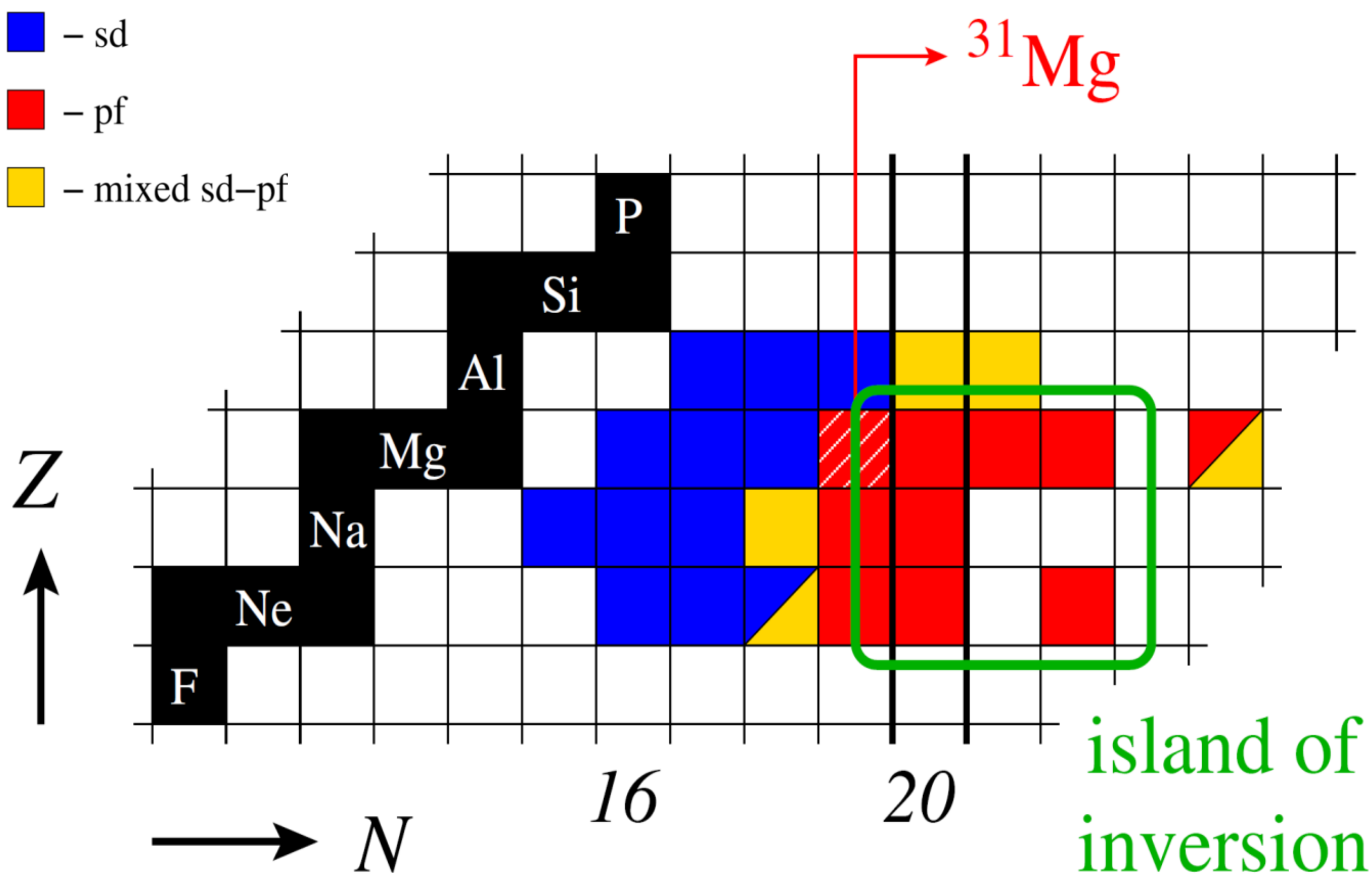

Nuclear structure studies through in-flight measurements

Today

- Method: Coulomb excitation at relativistic energies part II
- 2. Physics case: ‚More about shell model modifications‘
- 3. Physics case: ‚Neutron deficient Sn nuclei and the seniority scheme‘

ıkp

Coulomb excitation at relativistic energies

- Sommerfeld Parameter $\eta >> 1$

- adiabaticity parameter ξ

$$\xi \equiv \frac{\omega_{ph}}{\omega_{coll}} \equiv \frac{\Delta E}{\hbar} \tau_{coll} = \frac{\Delta E}{\hbar c} \frac{b}{\gamma\beta} \qquad \text{for } \xi = 1 \quad \Delta E_{max} = \frac{\gamma\beta\hbar c}{b_{min}}$$

- higher excitation energies at relativistic energies
- access to GDR range 10 - 20 MeV

Coulomb excitation: $^{56}Cr \rightarrow {}^{197}Au$

E/A	5 AMeV	60 AMeV	130 AMeV	500 AMeV
Adiabaticity parameter	0.6	0.17	0.11	0.05
E_{max}	1.6 MeV	5.7 MeV	8.6 MeV	18.6 MeV

Coulomb excitation cross section

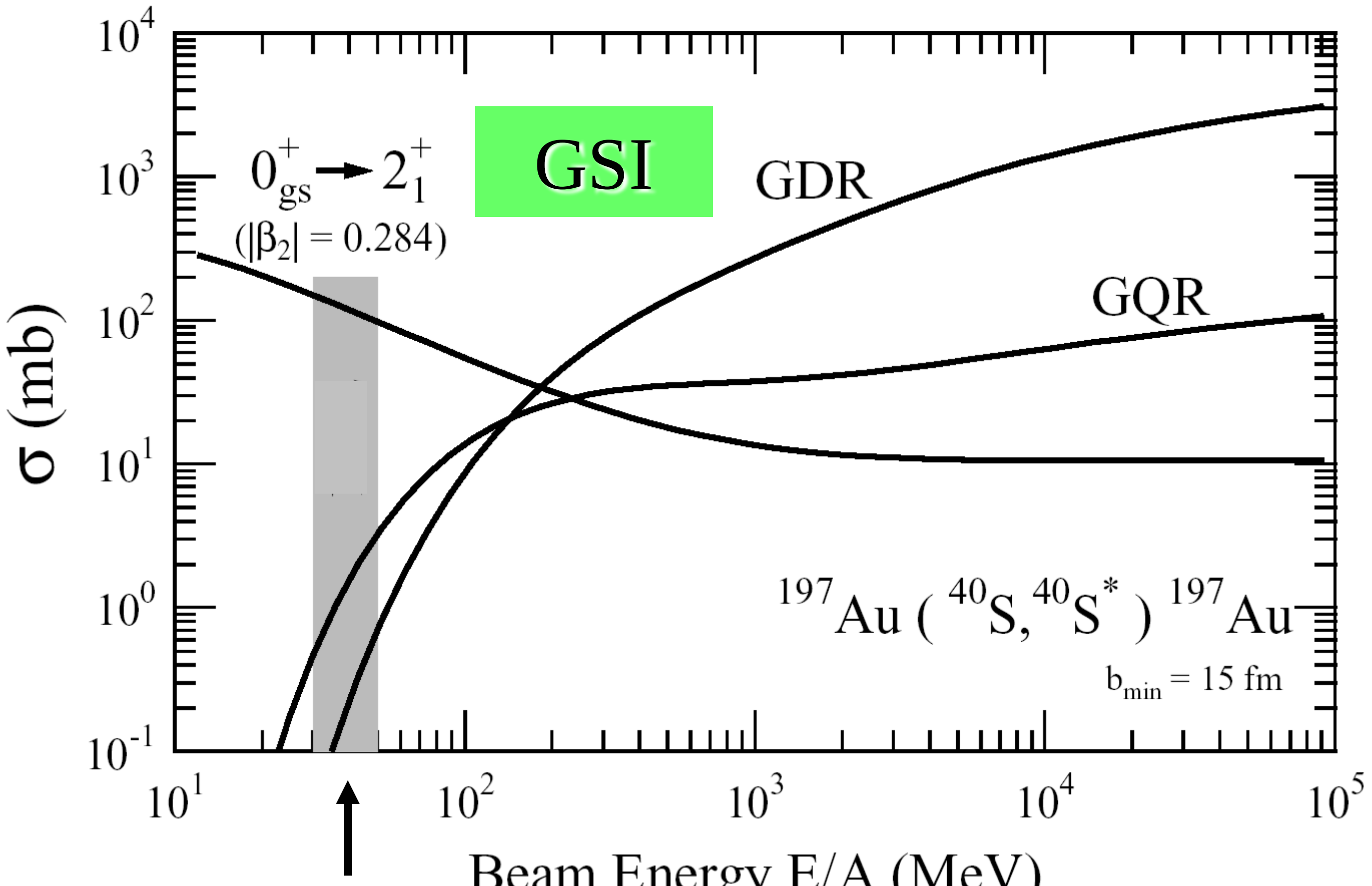

GANIL, NSCL, RIKEN

RareISotopeINvestigation at GSI

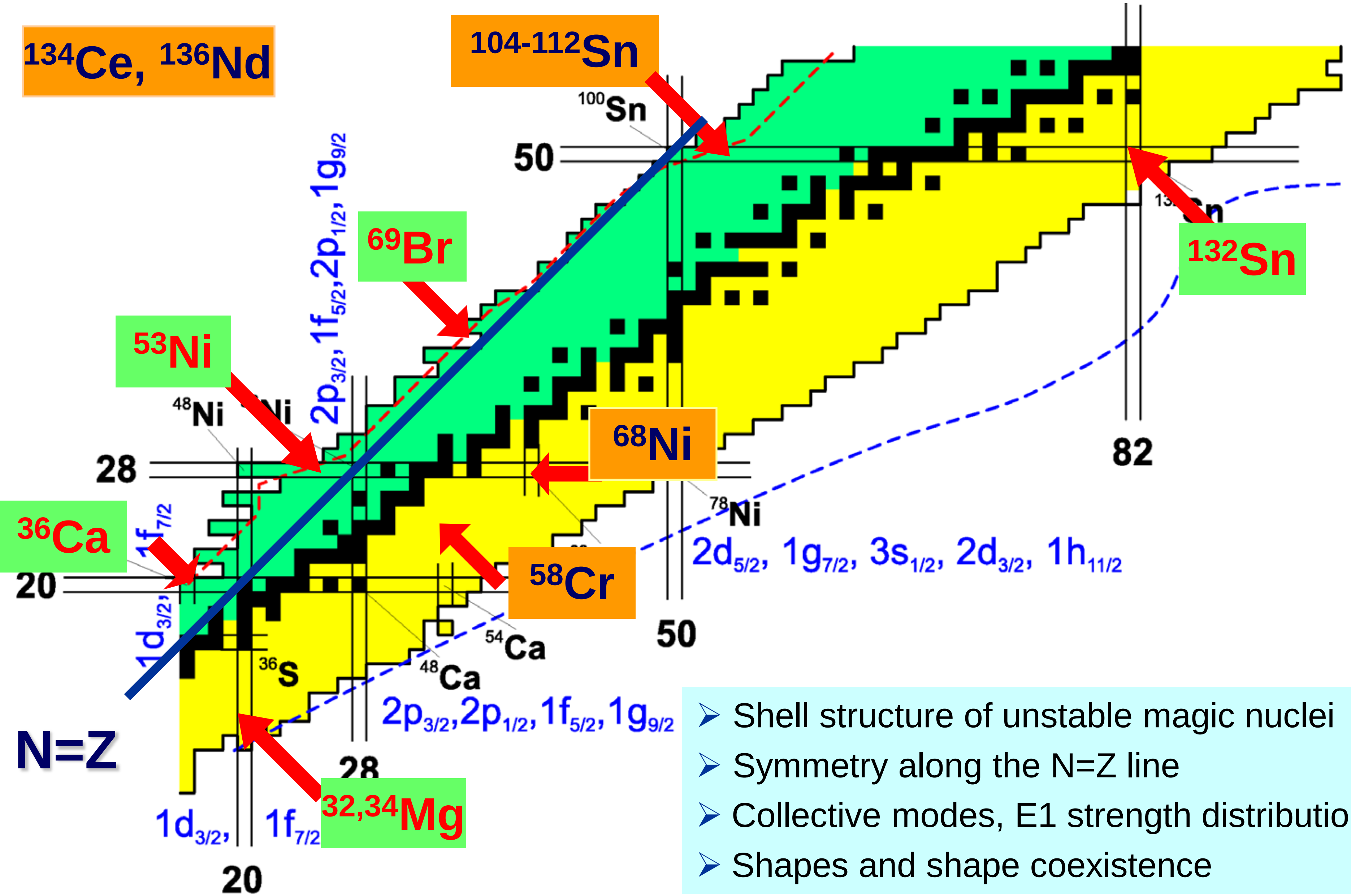

- Shell structure of unstable magic nuclei
- Symmetry along the N=Z line
- Collective modes, E1 strength distribution
- Shapes and shape coexistence

Relativistic beams at GSI

accelerators:

- UNILAC (injector) - E<15 AMeV
- SIS - E < 1 AGeV

beams:

- All ion species up to ^{238}U
- Currents:

  ^{238}U - 2* 10^8 pps

  medium mass nuclei- 10^9 pps

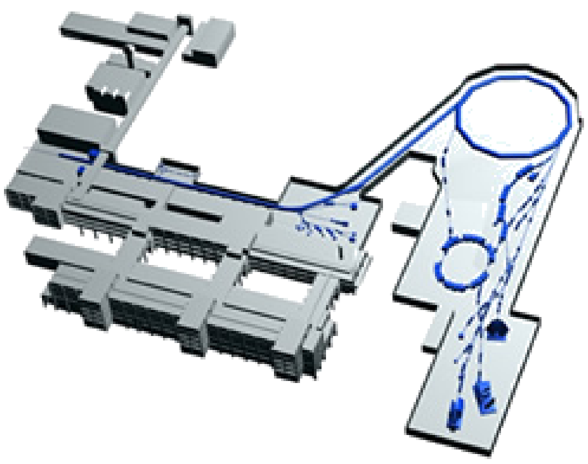

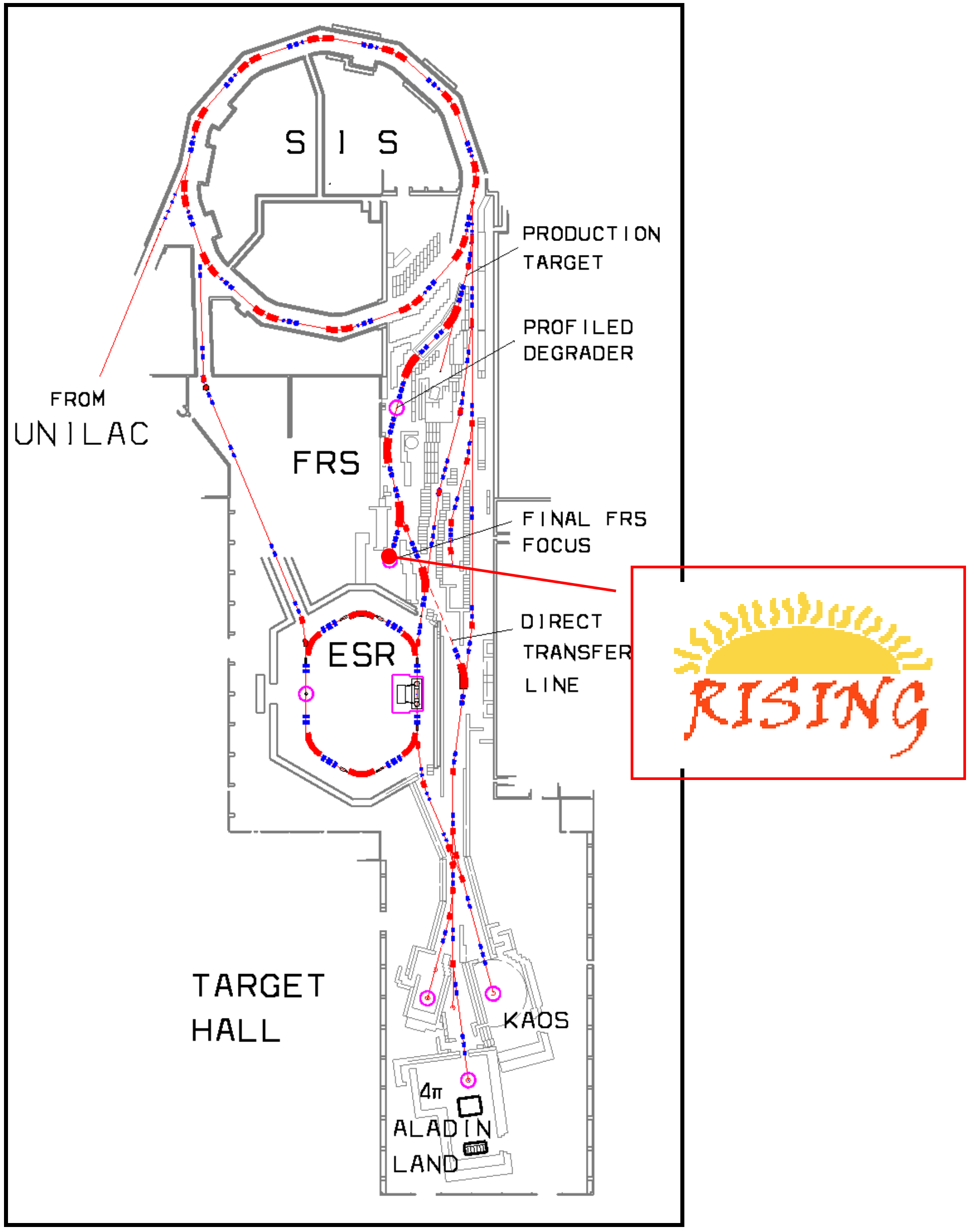

High resolution γ-spectroscopy at the FRS

FRS provides secondary radioactive ion beams:

- fragmentation and fission of primary beams
- high secondary beam energies: 100 – 500 MeV/u
- fully stripped ions

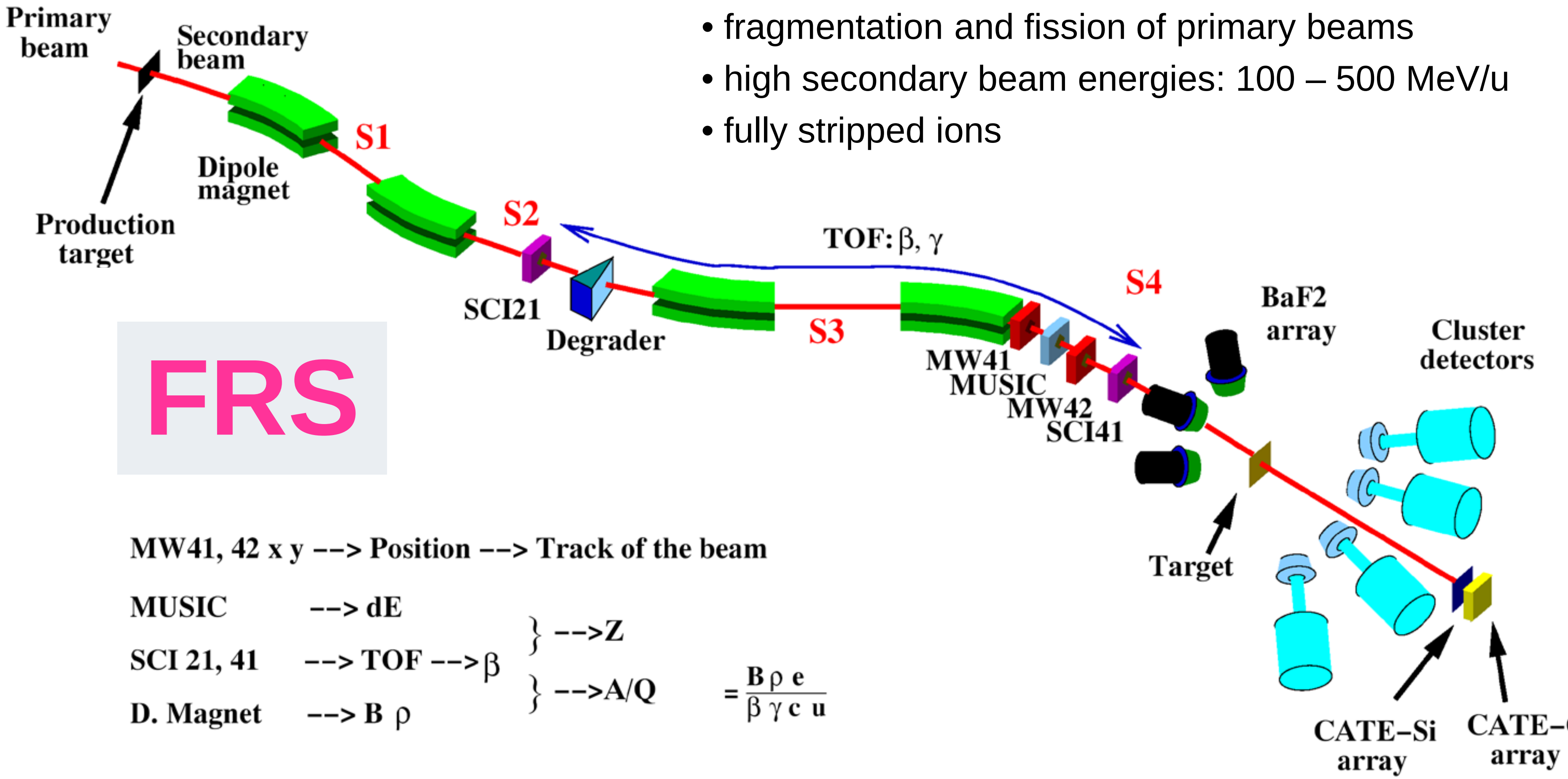

FRS

RISING

γ-spectroscopy at relativistic energies

High cross sections

- Coulomb excitation
- Secondary fragmentation

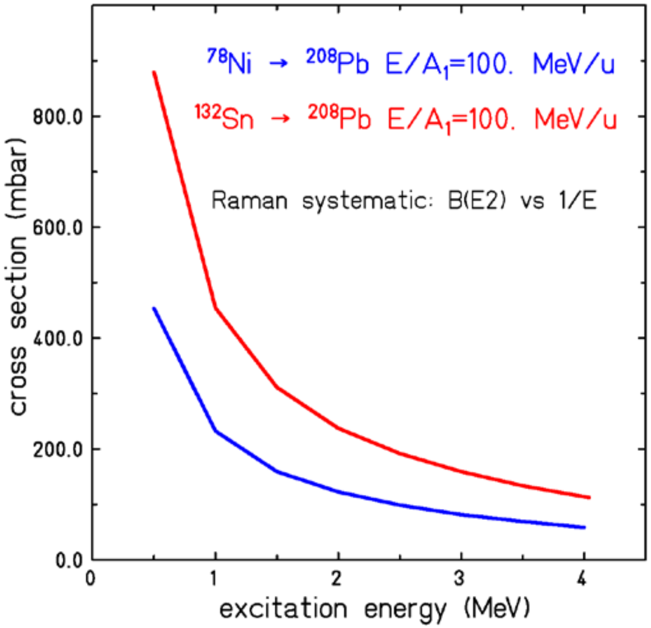

Thick targets

Lorentz boost of γ-rays

- Doppler shift
- Gain in geometrical efficiency
- Doppler broadening

Doppler broadening

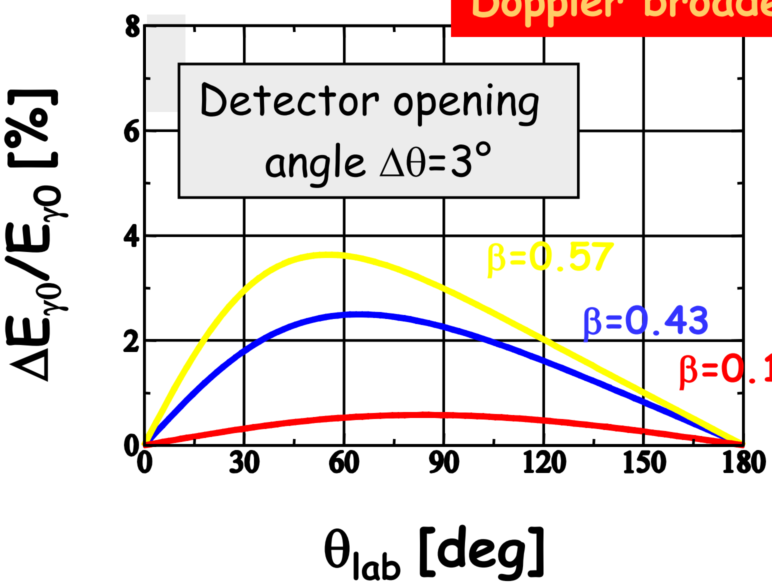

Atomic background, a limiting factor

- X-rays from target atoms
- Radiative electron capture
- Primary Bremsstrahlung
- Secondary Bremsstrahlung
- σ (atomic) ~ 10000 * σ (nuclear)

High energetic reactions

In-beam γ-spectroscopy at relativistic energies

Disadvantage

Doppler shift

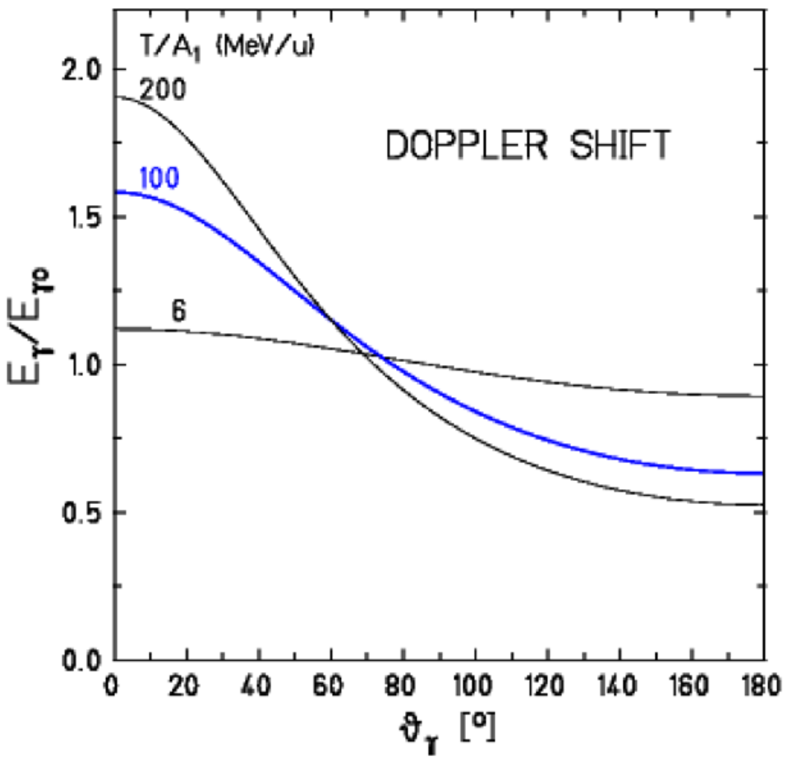

Doppler broadening

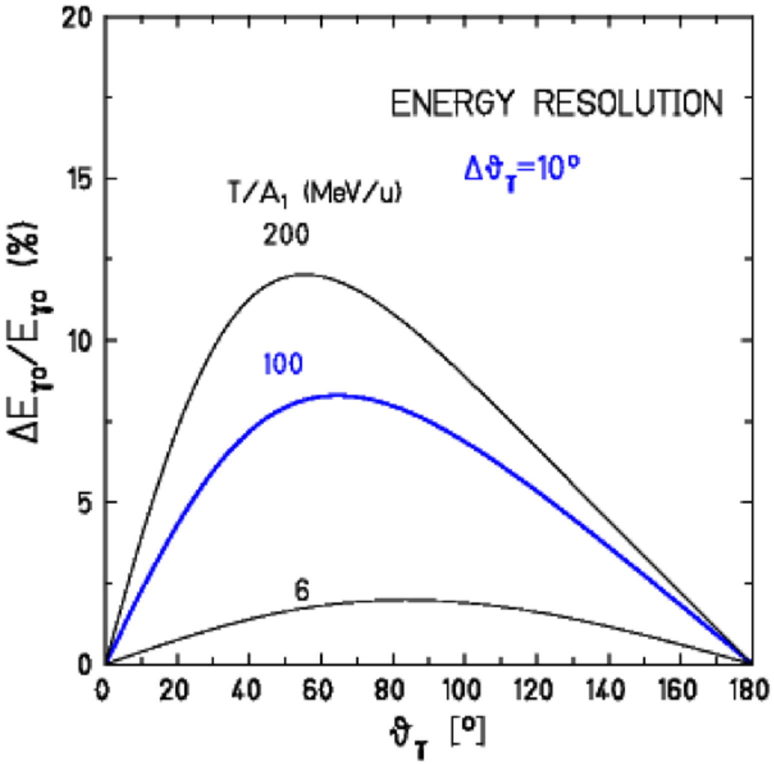

Rel. HPGe energy resolution: 0,18 %

In-beam γ-spectroscopy at relativistic energies

Lorentz transformation
- foreward boost
  => efficiency
- angular distribution

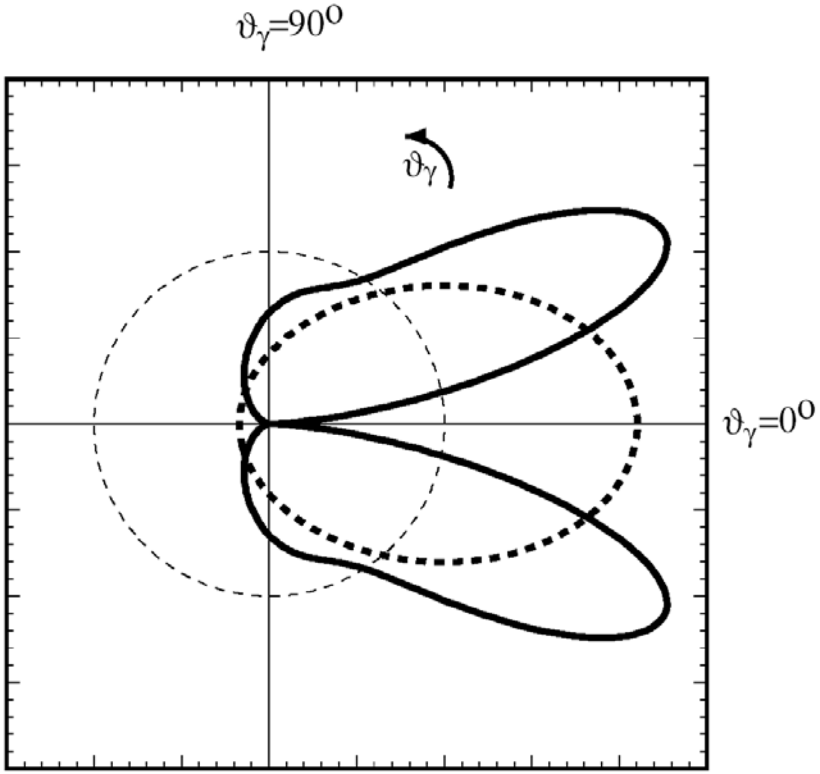

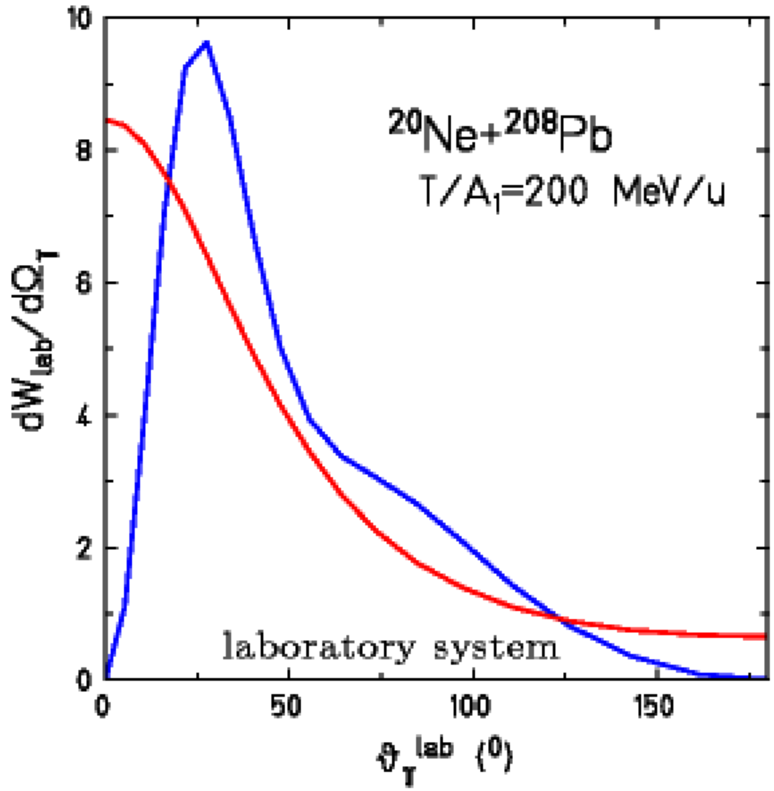

In-beam γ-spectroscopy at relativistic energies

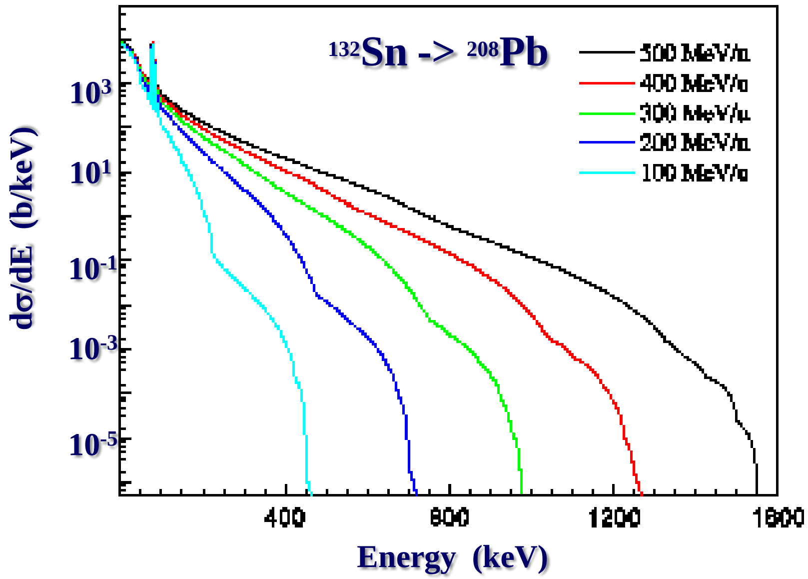

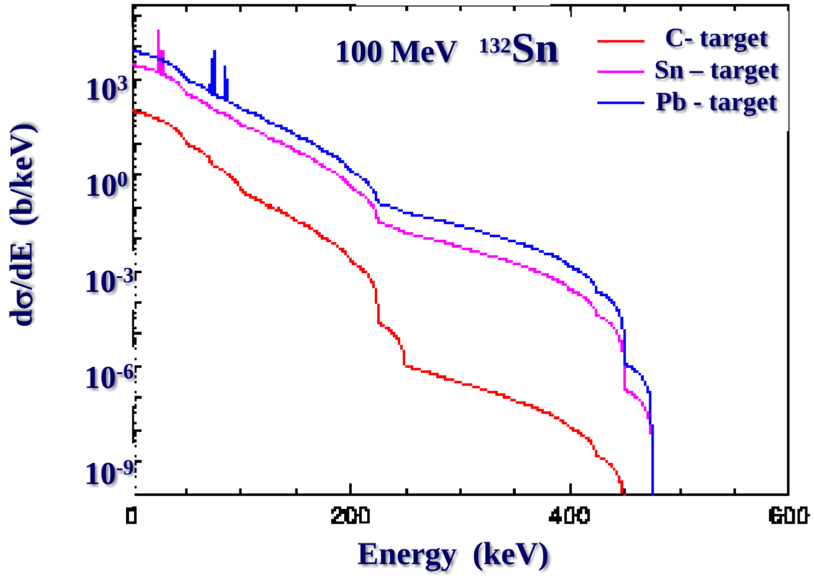

Atomic Background

- X-ray

- Radiative electron capture
(capture of target electrons into bound states of projectile)

- Primary Bremsstrahlung
(capture of target electrons into continuum states of projectile)

- Secondary Bremsstrahlung
(stopping of high energy electrons in the target)

EUROBALL-Cluster array

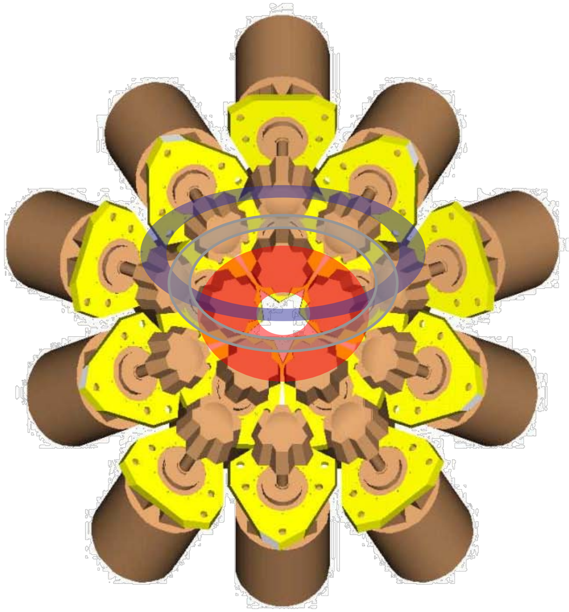

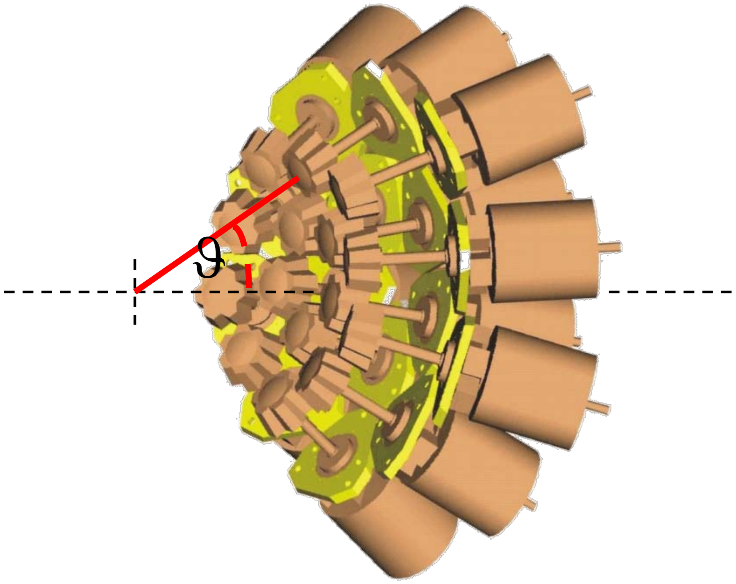

15 EUROBALL

Cluster detectors

without ACS

105 Ge crystals

Ring	Angle [deg]	Distance [mm]	Resolution [%]	Efficiency [%]
1	15.9	700	1.00	1.00
2	33.0	700	1.82	0.91
3	36.0	700	1.93	0.89
		Total:	1.56	2.81

H.J. Wollersheim et al.; NIM A 537 (2005) 637

Ge-Cluster detectors

Seven encapsulated Ge crystals in common vacuum
Efficiency ~60 % each, hexagonal tapered

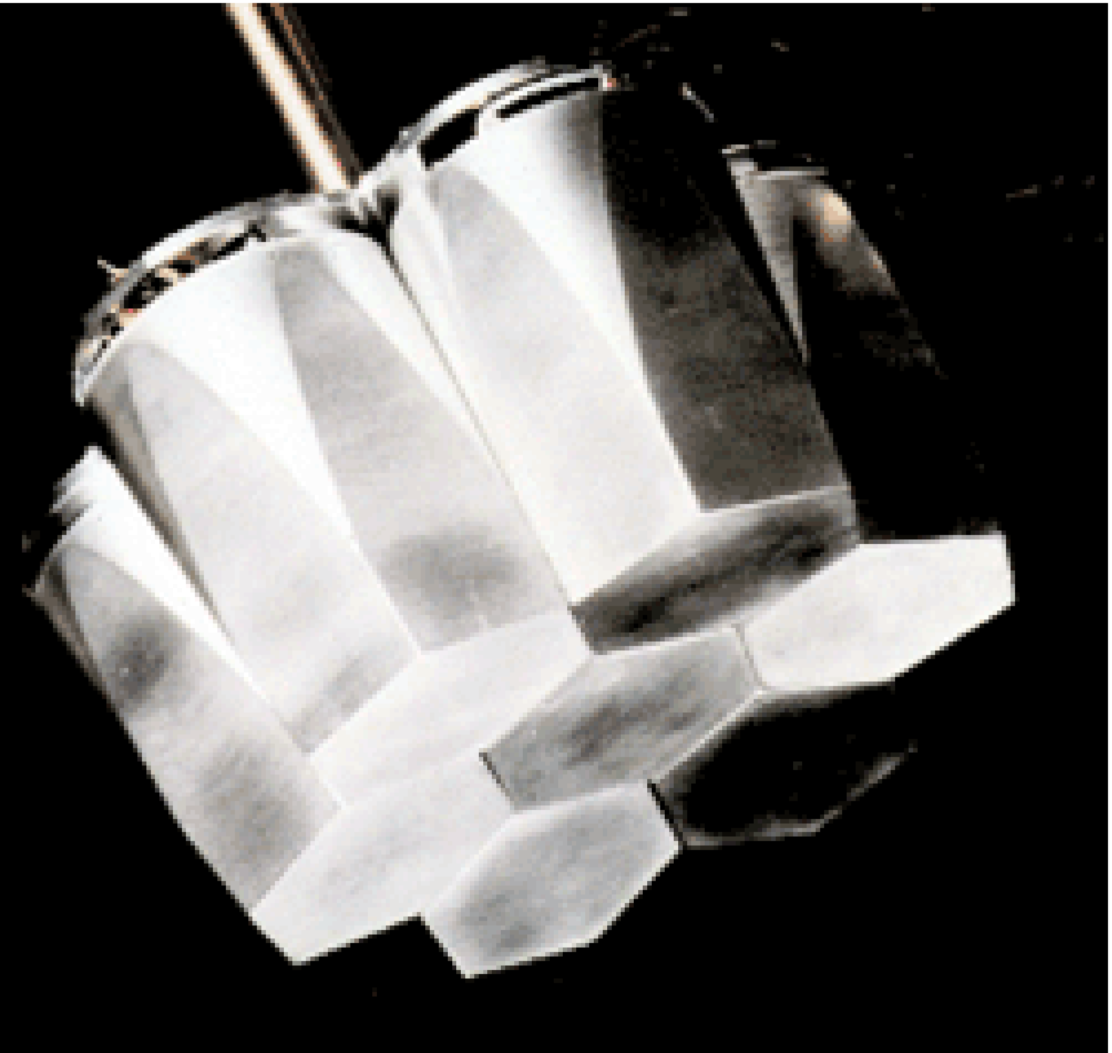

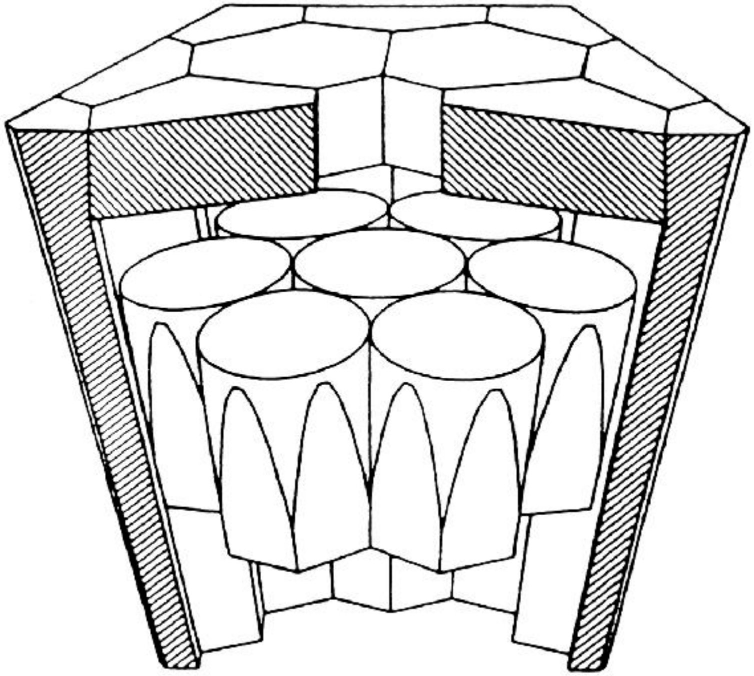

RISING experimental setup

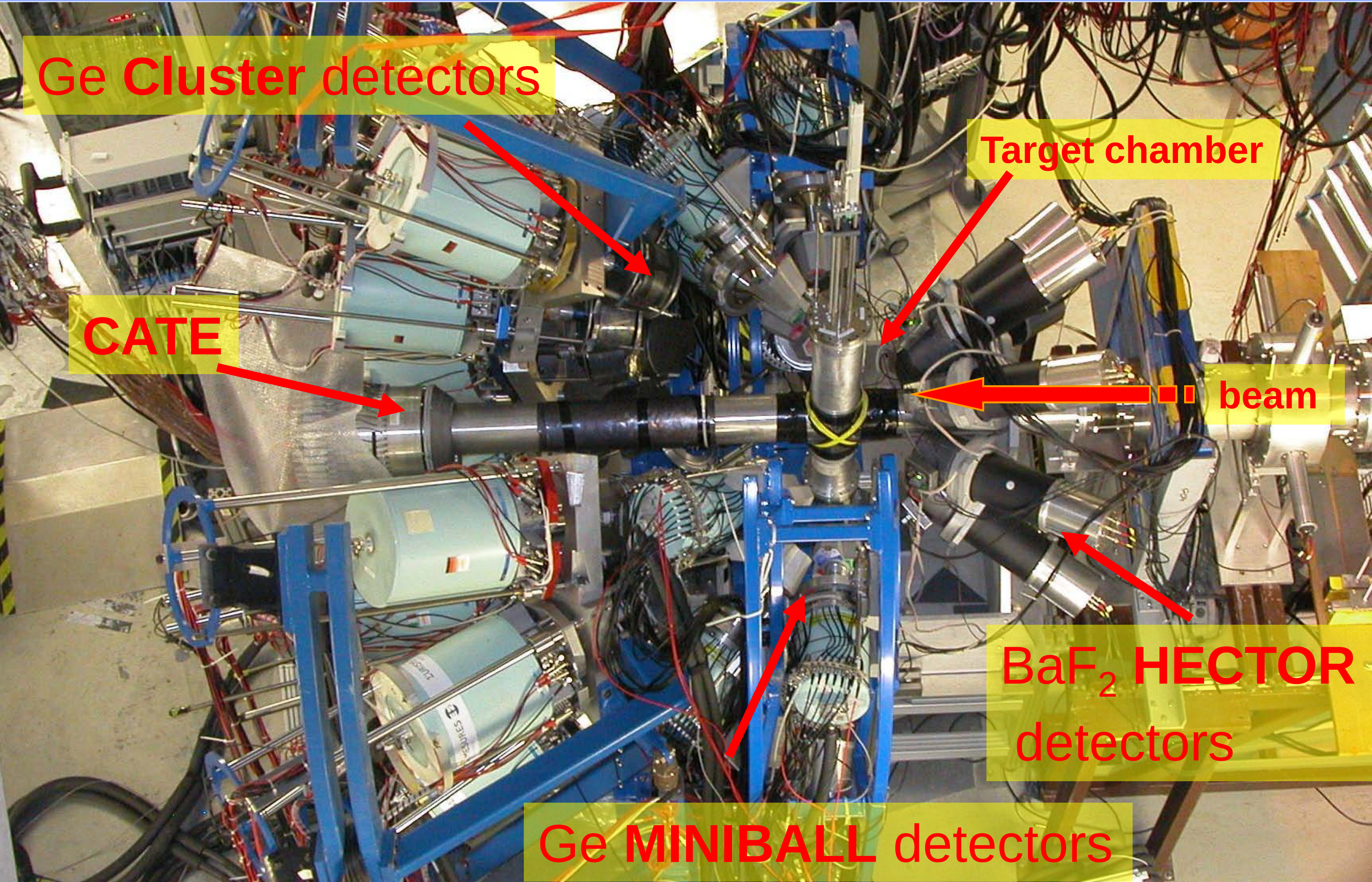

New Shell Structure at N>>Z

Mirror symmetry of (sub)shell closures

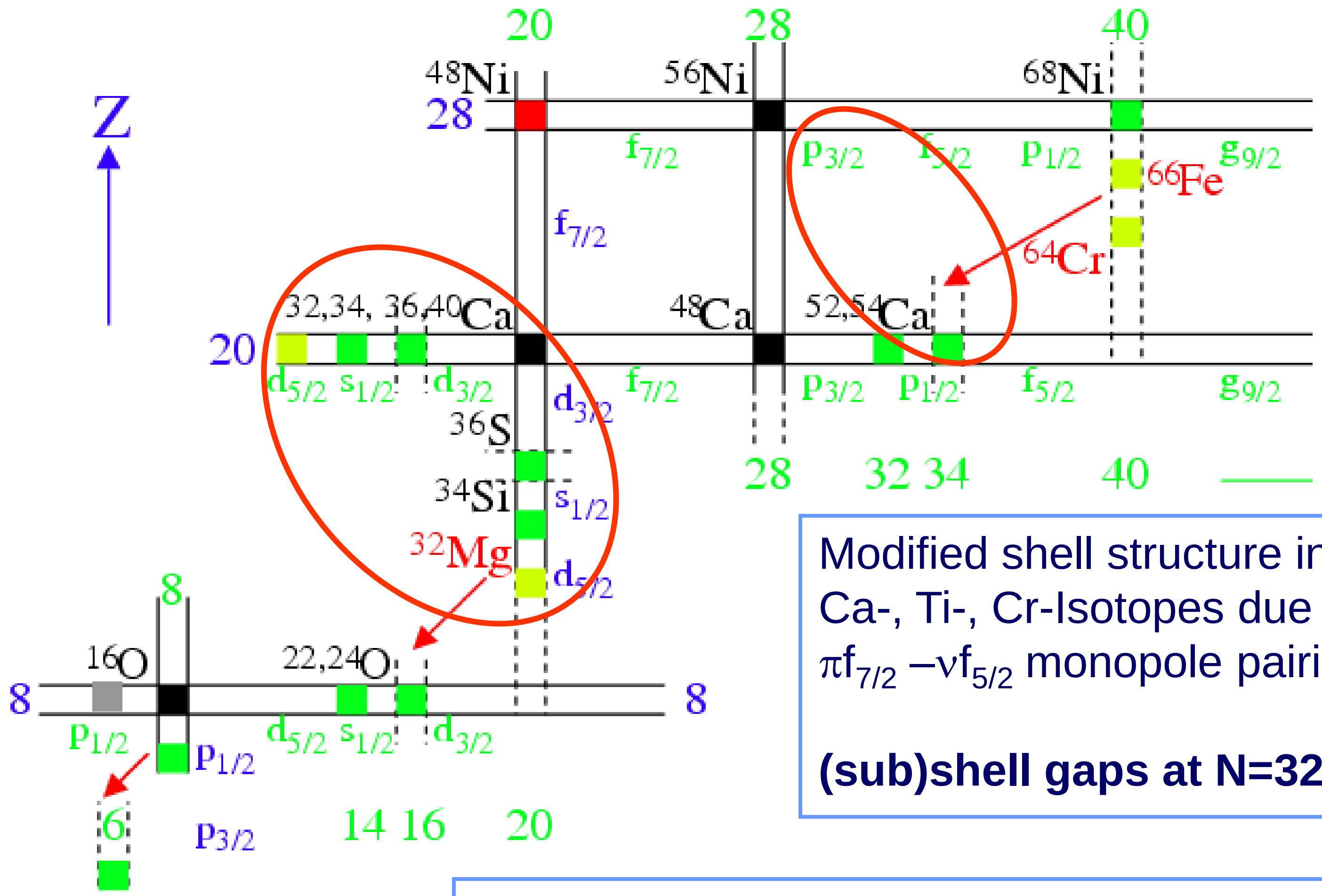

Modified shell structure in neutron-rich Ca-, Ti-, Cr-Isotopes due to weaker $\pi f_{7/2} - \nu f_{5/2}$ monopole pairing interactions?

(sub)shell gaps at N=32 and N=34?

Z=14(16) shell stabilisation and Z=12 shell quenching in N=20 isotones.
(sub)shell gaps at N=14,16 for Ca isotopes?

New Shell Structure at N>>Z
Relativistic Coulex in N=28-34 Nuclei

- Large scale shell modell calculations
  - *GXPF1, GXPF1A*
    M.Honma et al,
    Phys. Rev. C65(2002)061301

  - *KB3G*
    E.Caurier et al,
    Eur.Phys.J. A 15, 145 (2002)

- Transition matrix elements
  - B(E2) in ^{52,54,56}Ti (MSU)
  - B(E2) in ^{54,56,58}Cr (GSI)

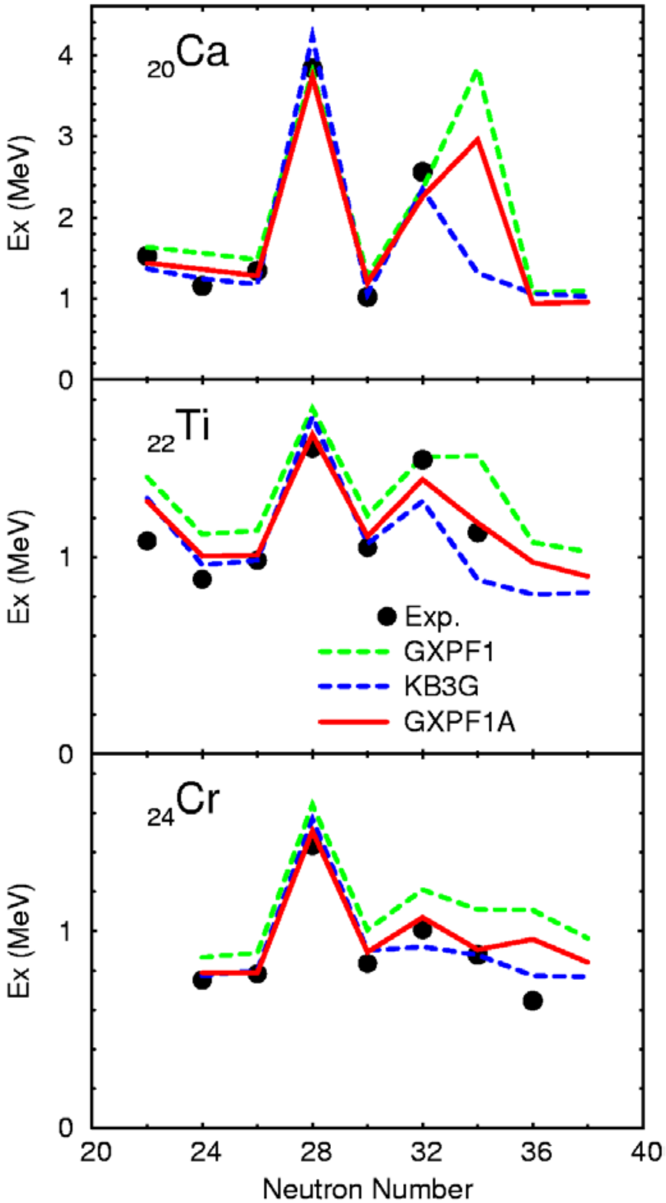

RI beam: fragment identification and tracking

Primary beam ^{86}Kr, 480 MeV/u, 10^9 p/sec

Secondary beams, 136 MeV/u:

- ^{54}Cr: 4 x 10^3 part./s, 22 h, 45% ^{54}Cr
- ^{56}Cr: 1 x 10^3 part./s, 20 h, 35% ^{56}Cr
- ^{58}Cr: 3 x 10^2 part./s, 55 h, 25% ^{58}Cr

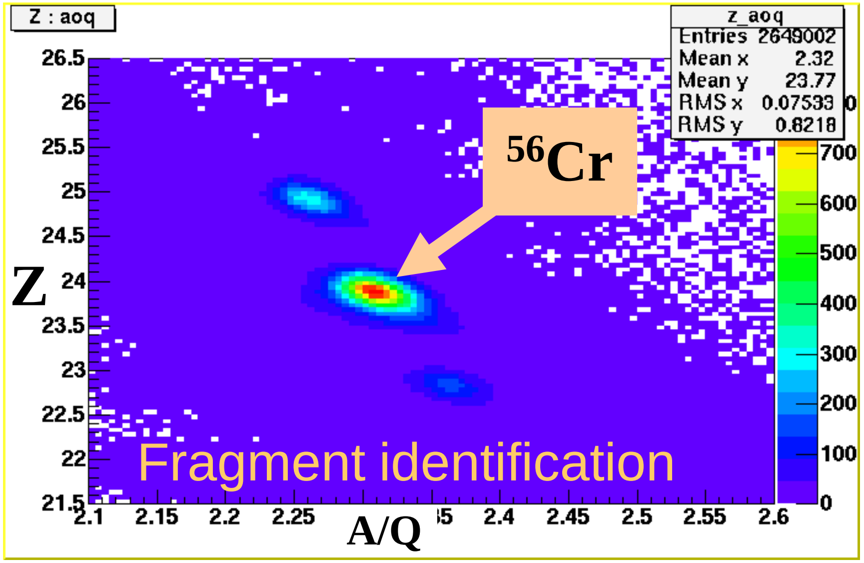

Tracking before target

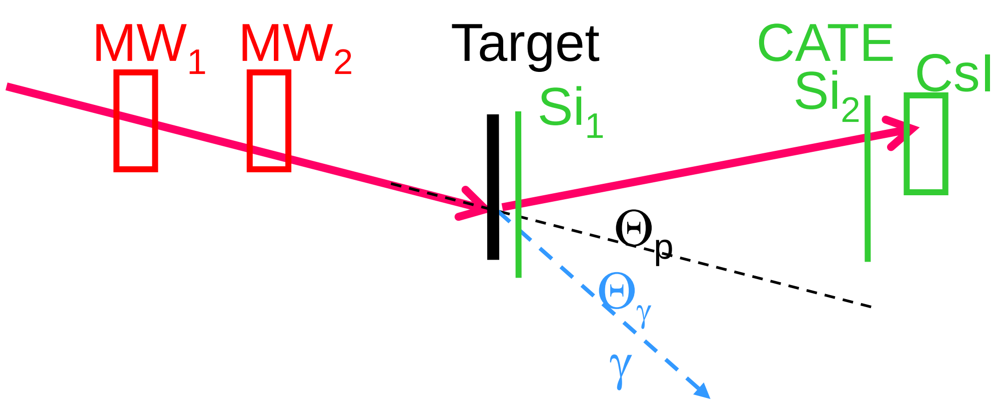

Multiwire extrapolation to target

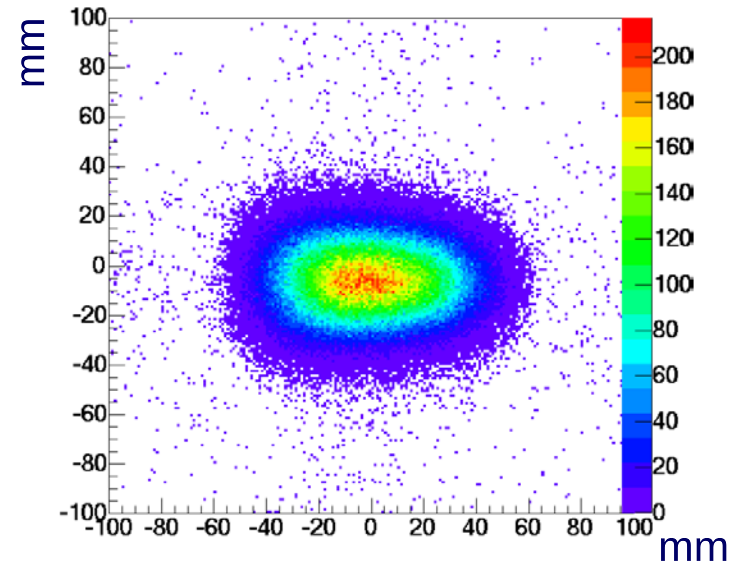

CAlorimeter TElescope CATE
Particle Identification and Tracking after Target

R. Lozeva et al, NIM B, *204 (2003) 678*

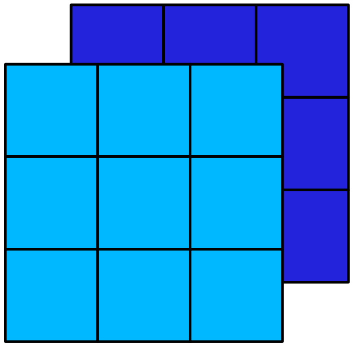

E
- **CsI detectors**
- **Z identification**

ΔE
- **0.3 mm thick Si detectors**
- **Z identification**
- **Position sensitive**

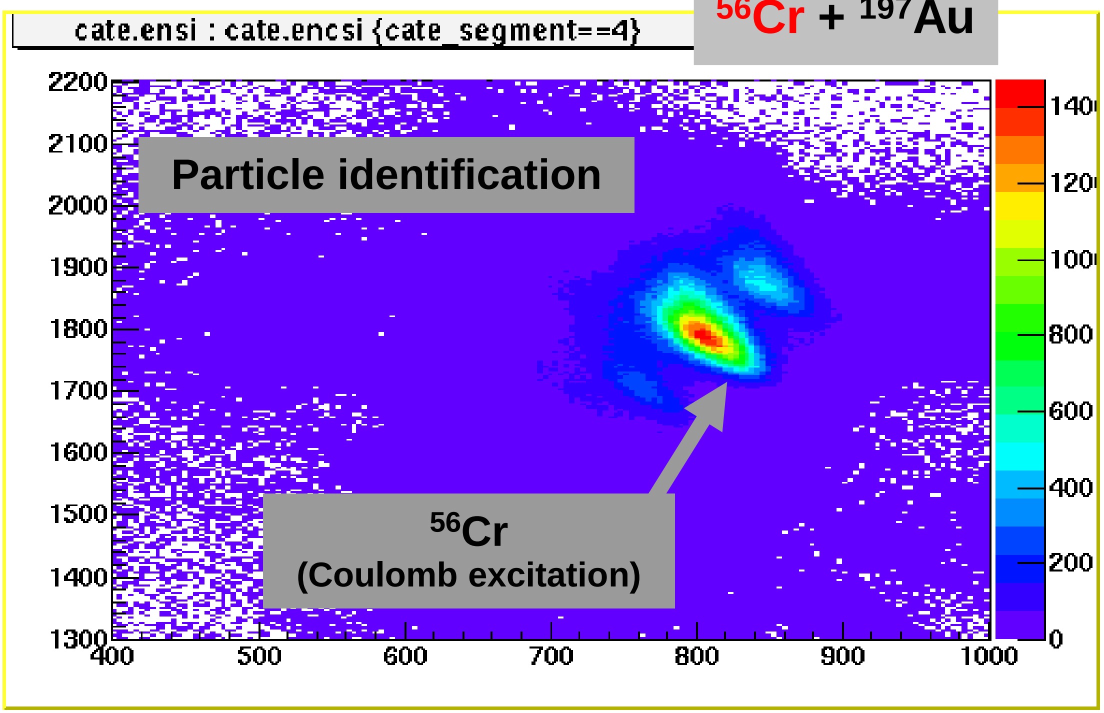

Tracking after target

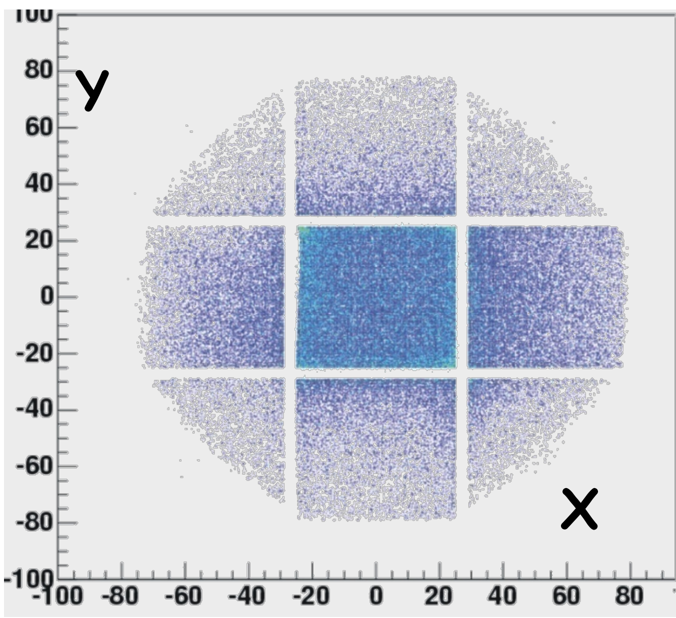

Tracking: - Doppler correction
- scattering angle

- velocity v/c from TOF (event-by-event)
- tracking of ions: γ-ray emission angle

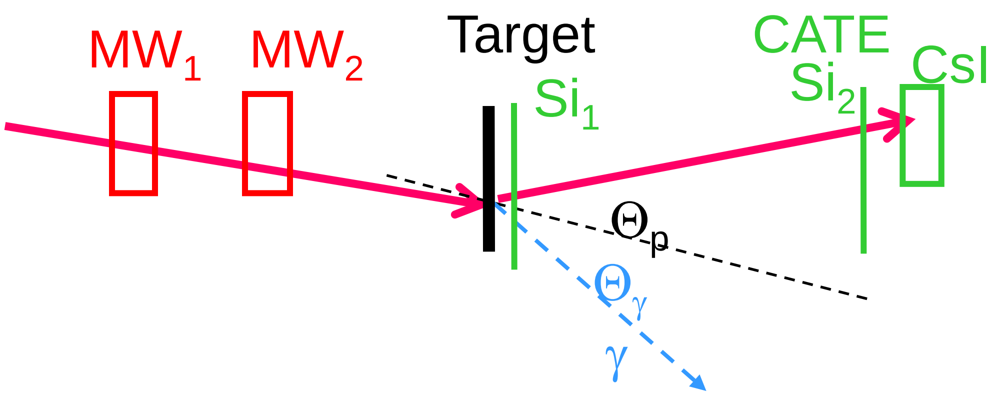

ð γ-ray energy resolution

ð scattering angle

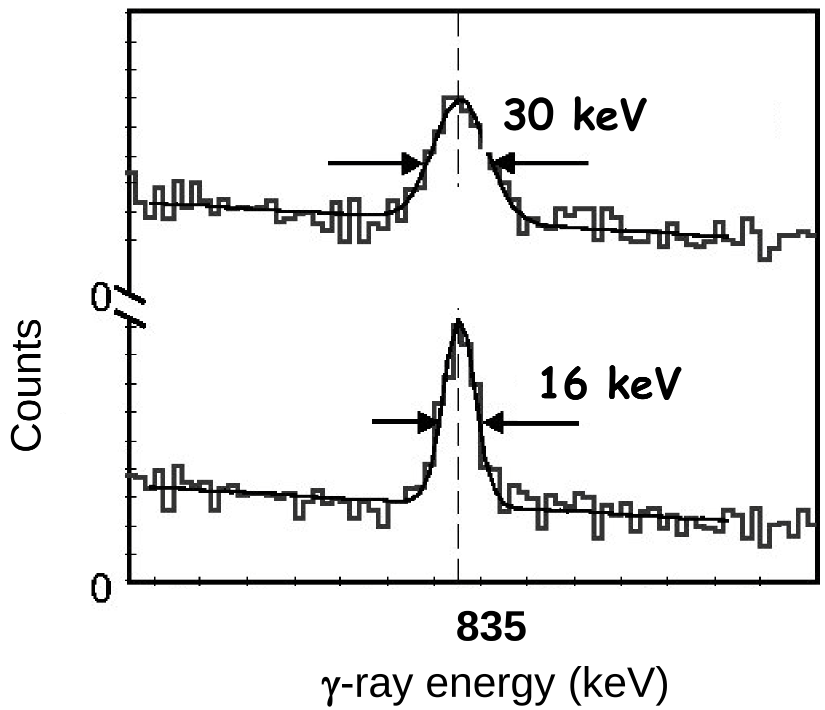

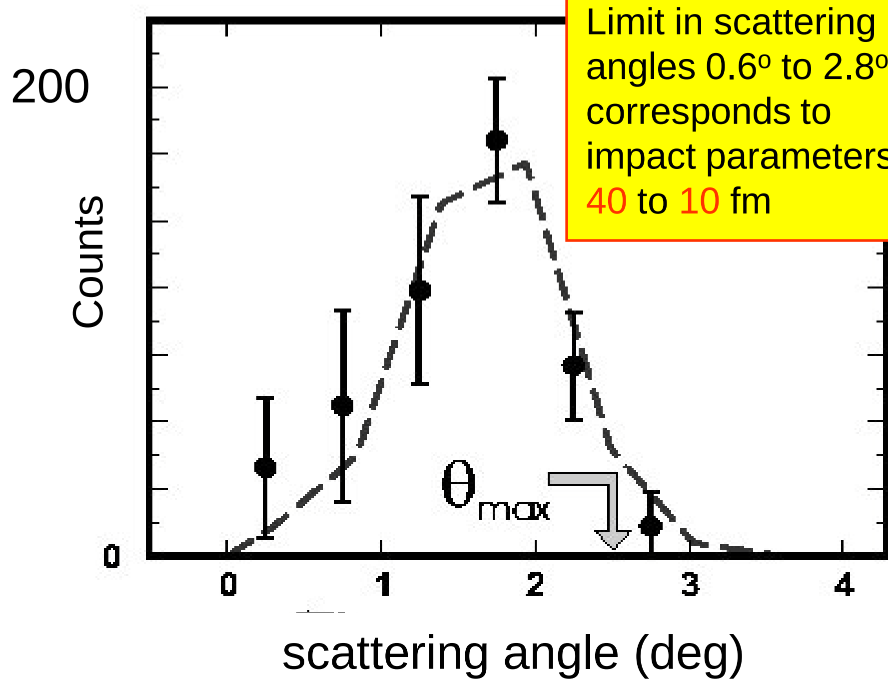

Limit in scattering angles 0.6º to 2.8º corresponds to impact parameters: 40 to 10 fm

New Shell Structure at N>>Z
Relativistic Coulex in N=28-34 Nuclei

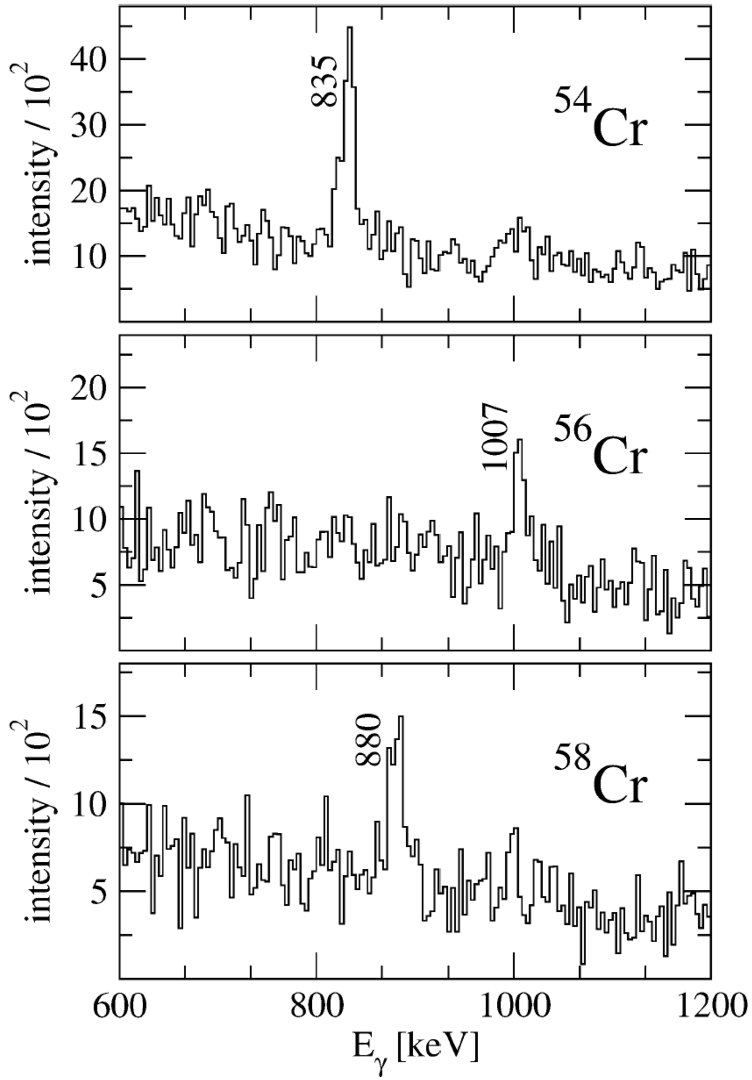

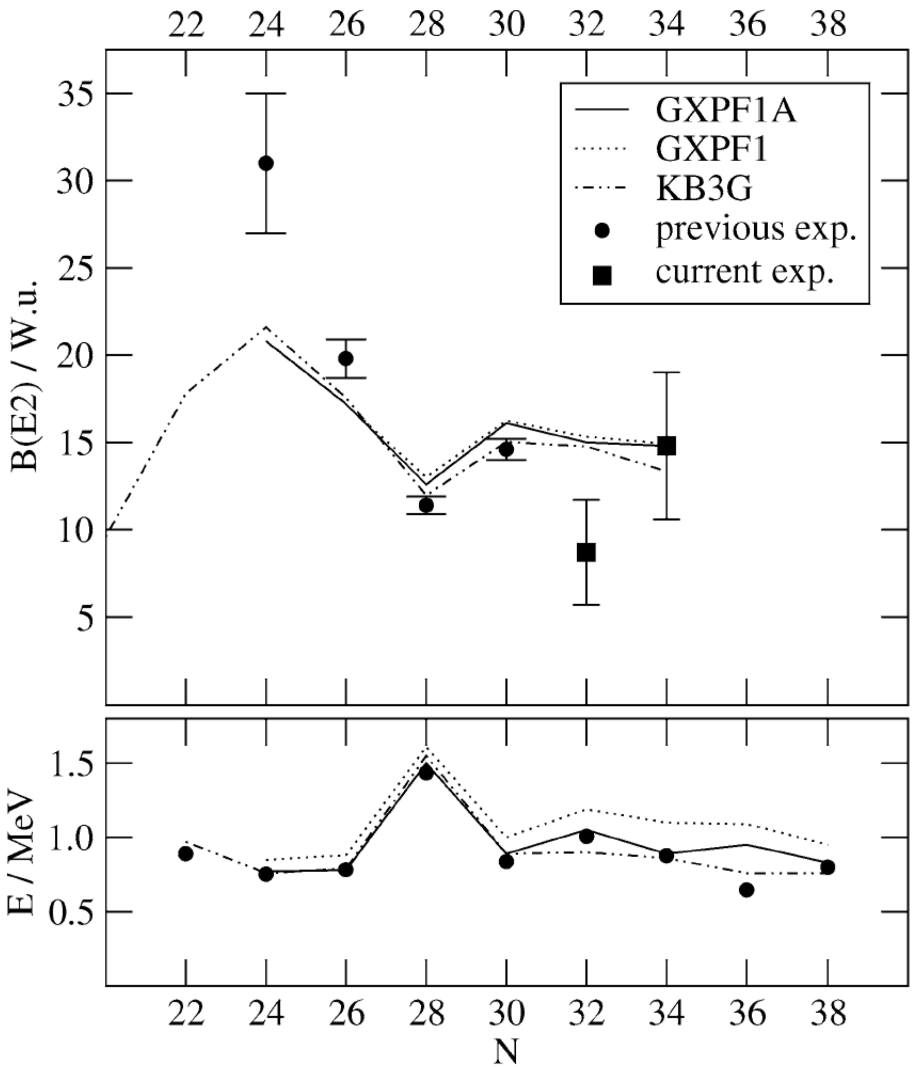

A. Bürger et al., Phys. Lett B 622, 29 (2005)

Comparison with $^{52,54,56}Ti$

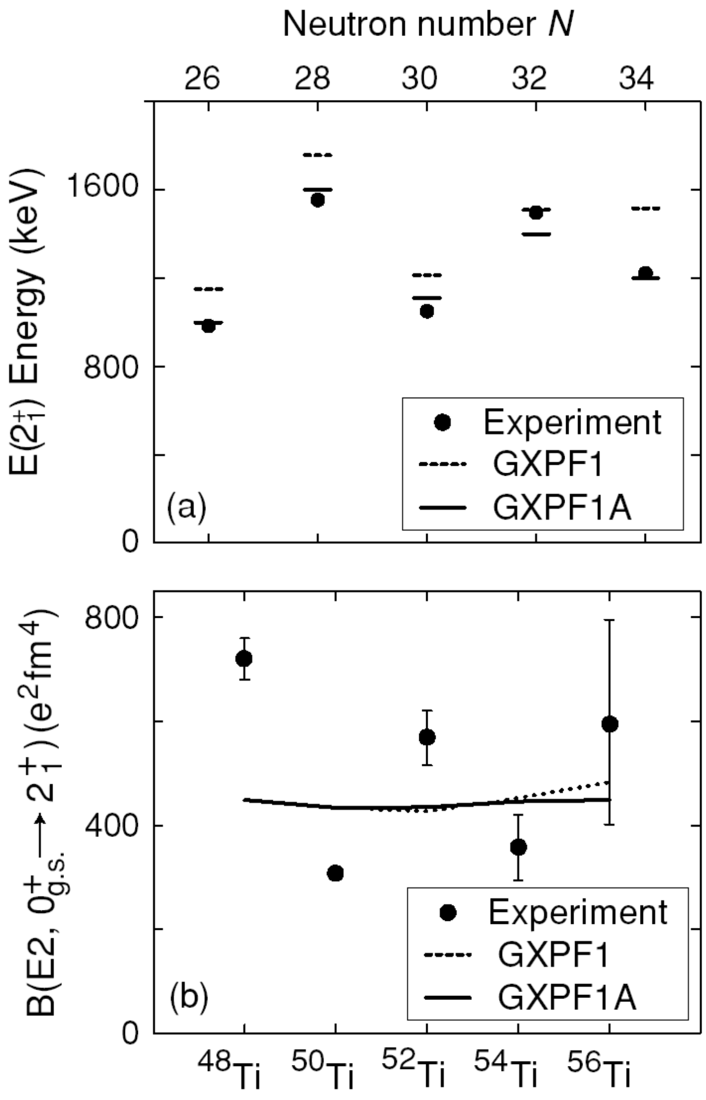

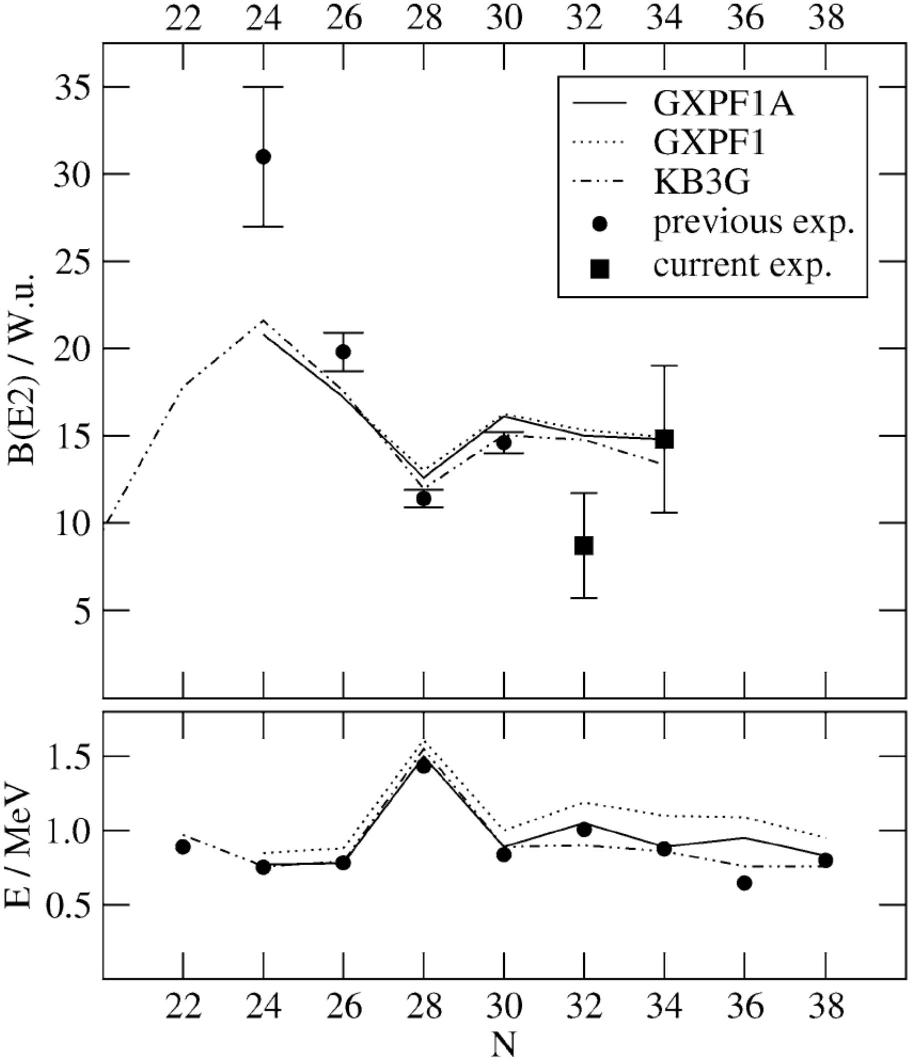

D.-C. Dinca et al., Phys Rev. C 041302(R) (2005)

Stable beam lifetime measurement in ^{56}Cr

Recoil Distance Doppler Shift
Plunger Method

Doppler shift:
$\Delta E = E_0 \cdot v/c \cdot \cos(\theta)$

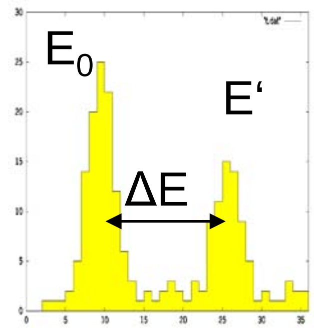

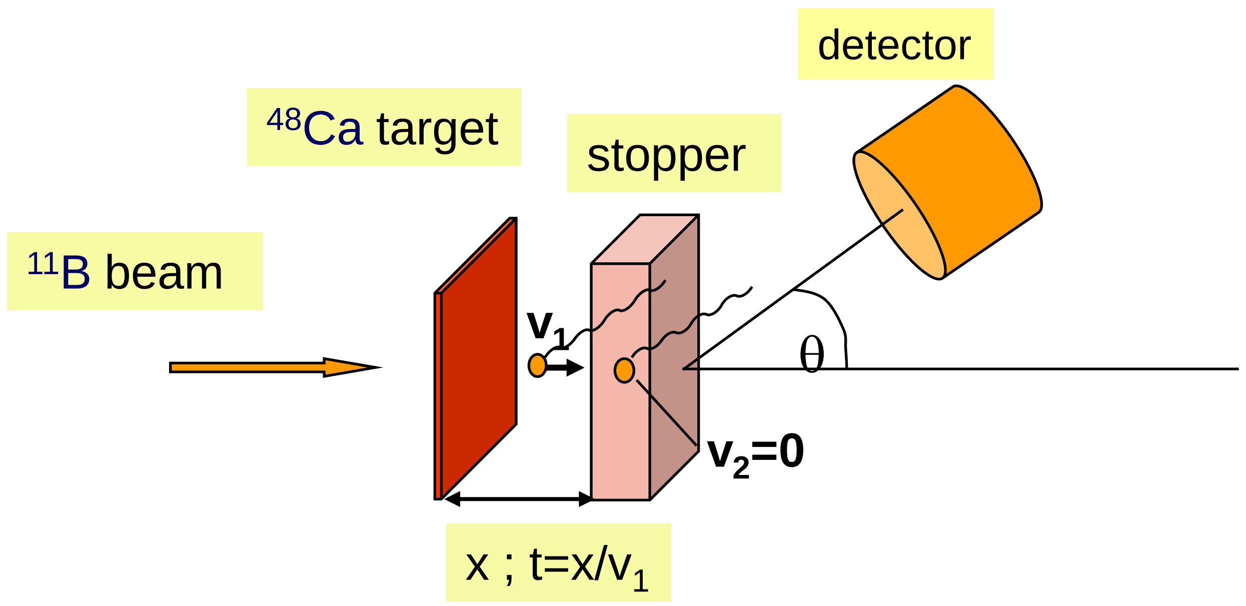

^{48}Ca(^{11}B,*p2n*)^{56}Cr @ 30 MeV
Cologne tandem accelerator

Set up: Cologne plunger
Foreward: EUROBALL Cluster
Backward: 5 Ge-detector

lifetime measurement in ^{56}Cr

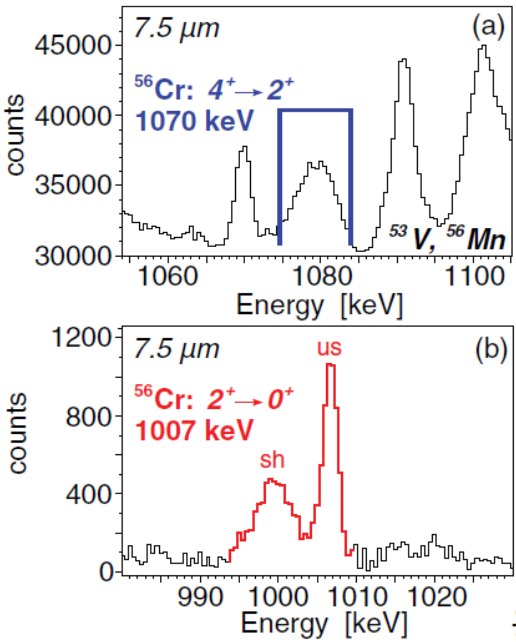

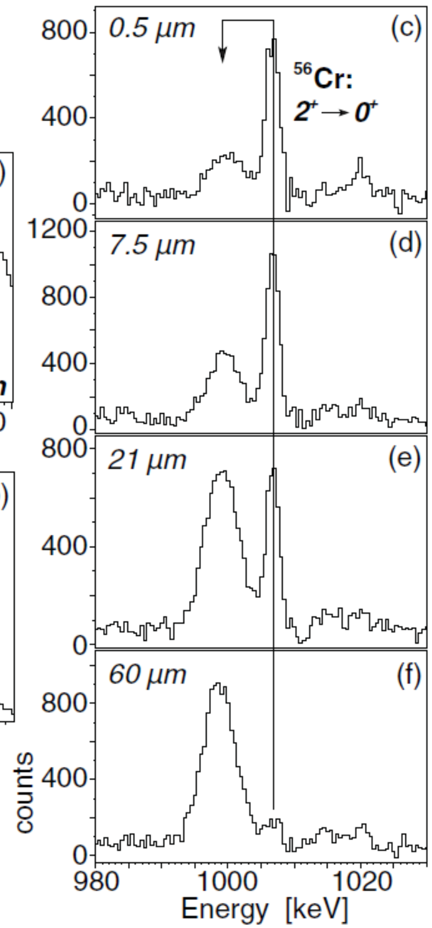

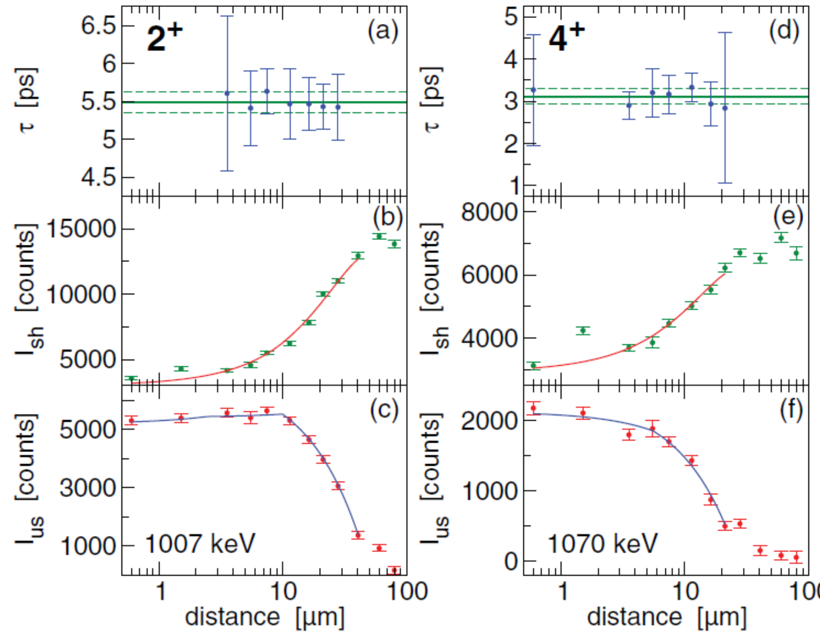

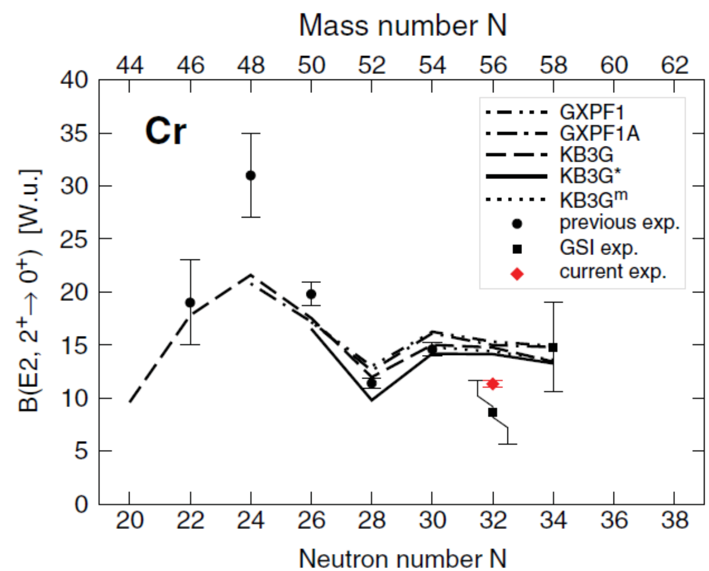

M. Seidlitz et al. Phys Rev.C 84, 034318 (2011)

lifetime measurement in ^{56}Cr

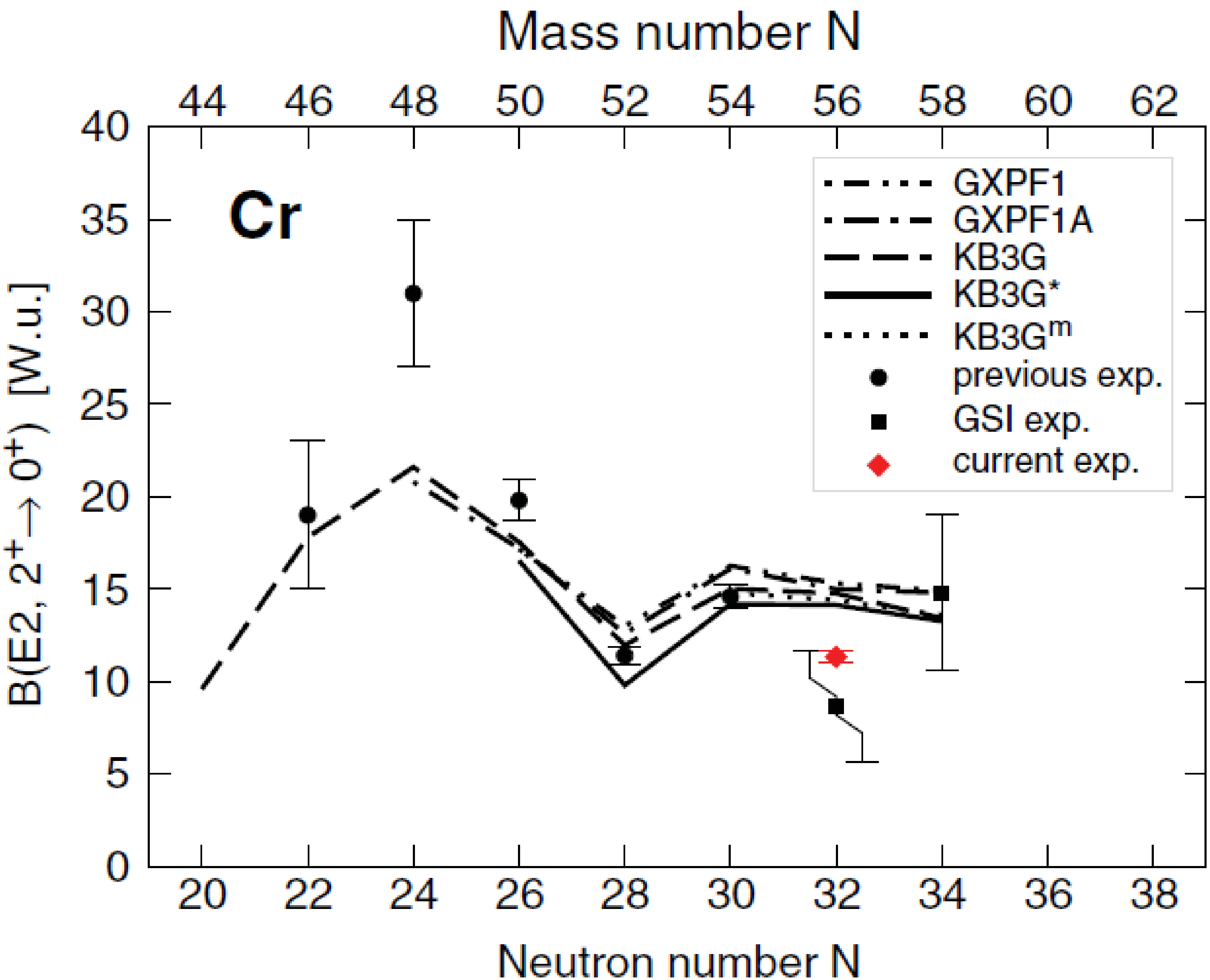

M. Seidlitz et al. Phys Rev.C 84, 034318 (2011)

New Shell Structure at N»Z
- the mirror point of view -

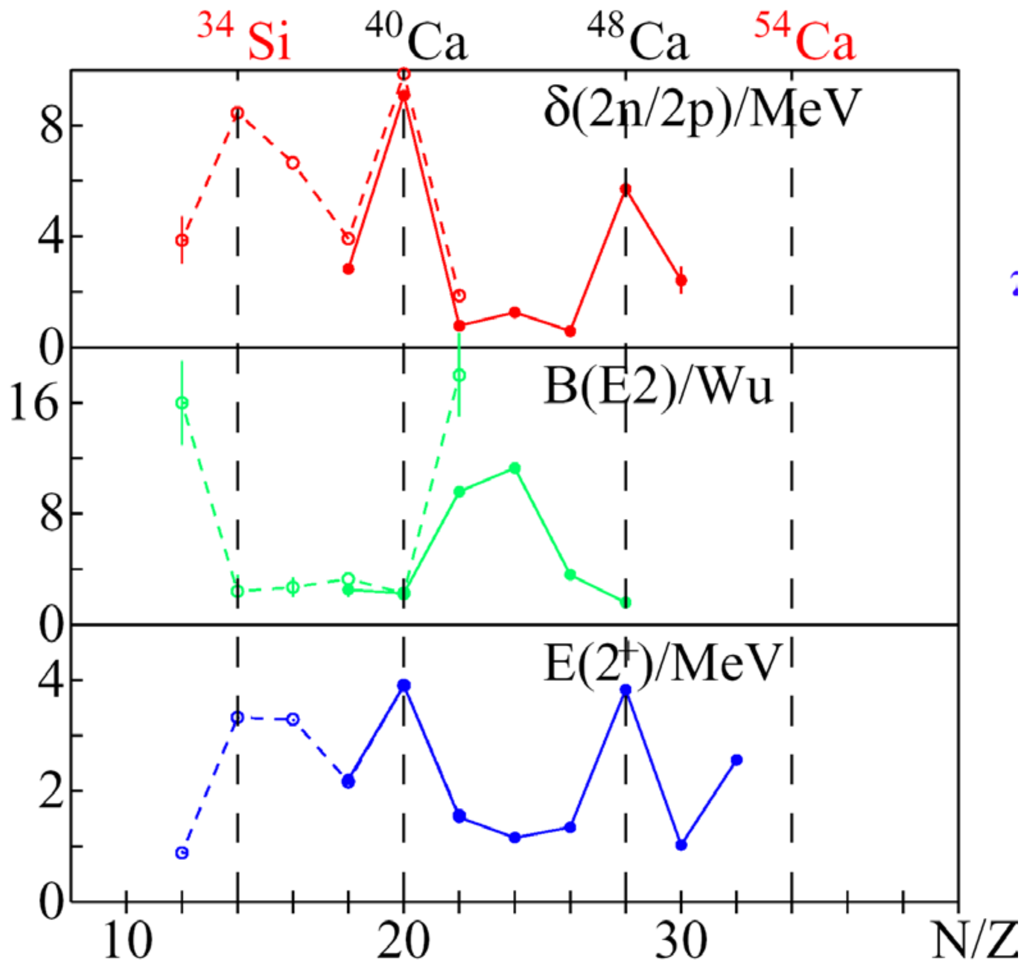

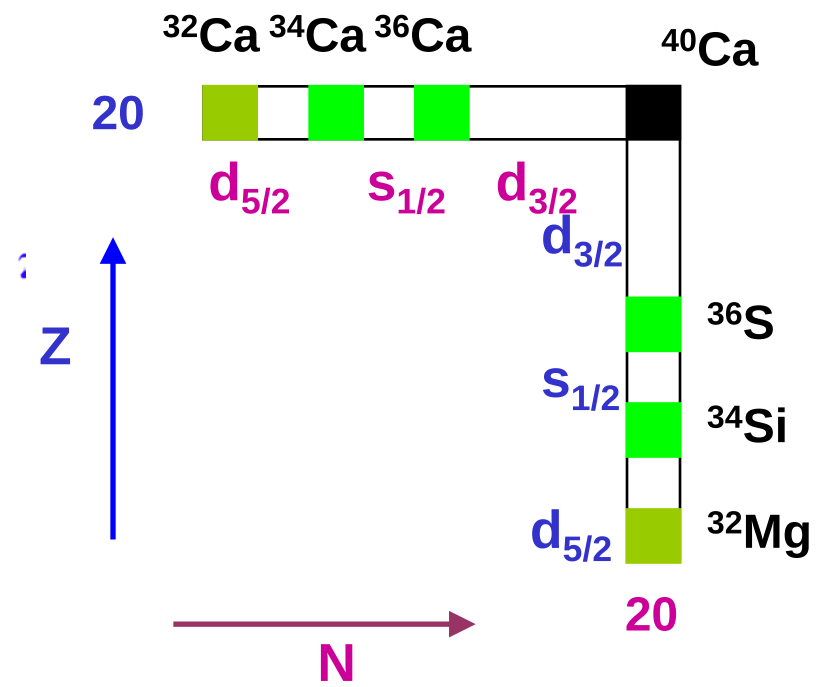

Is N,Z=14(16) shell stabilisation and N=20 shell quenching symmetric in isospin projection T_z?

Isospin symmetry in Z=20 isotopes
- excited states in ^{36}Ca vs ^{36}S